NASA / CR-2000-210654

Theoretical Analysis of the Electron Spiral Toroid Concept

Jean-Luc Cambier and David A. Micheletti
MSE Technology Applications, Inc., Butte, Montana

December 2000

The NASA STI Program Office ... in Profile

Since its founding, NASA has been dedicated to the advancement of aeronautics and space science. The NASA Scientific and Technical Information (STI) Program Office plays a key part in helping NASA maintain this important role.

The NASA STI Program Office is operated by Langley Research Center, the lead center for NASA's scientific and technical information. The NASA STI Program Office provides access to the NASA STI Database, the largest collection of aeronautical and space science STI in the world. The Program Office is also NASA's institutional mechanism for disseminating the results of its research and development activities. These results are published by NASA in the NASA STI Report Series, which includes the following report types:

- TECHNICAL PUBLICATION. Reports of completed research or a major significant phase of research that present the results of NASA programs and include extensive data or theoretical analysis. Includes compilations of significant scientific and technical data and information deemed to be of continuing reference value. NASA counterpart of peer-reviewed formal professional papers, but having less stringent limitations on manuscript length and extent of graphic presentations.

- TECHNICAL MEMORANDUM. Scientific and technical findings that are preliminary or of specialized interest, e.g., quick release reports, working papers, and bibliographies that contain minimal annotation. Does not contain extensive analysis.

- CONTRACTOR REPORT. Scientific and technical findings by NASA-sponsored contractors and grantees.

- CONFERENCE PUBLICATION. Collected papers from scientific and technical conferences, symposia, seminars, or other meetings sponsored or co-sponsored by NASA.

- SPECIAL PUBLICATION. Scientific, technical, or historical information from NASA programs, projects, and missions, often concerned with subjects having substantial public interest.

- TECHNICAL TRANSLATION. English-language translations of foreign scientific and technical material pertinent to NASA's mission.

Specialized services that complement the STI Program Office's diverse offerings include creating custom thesauri, building customized databases, organizing and publishing research results ... even providing videos.

For more information about the NASA STI Program Office, see the following:

- Access the NASA STI Program Home Page at *http://www.sti.nasa.gov*

- E-mail your question via the Internet to help@sti.nasa.gov

- Fax your question to the NASA STI Help Desk at (301) 621-0134

- Phone the NASA STI Help Desk at (301) 621-0390

- Write to:
  NASA STI Help Desk
  NASA Center for AeroSpace Information
  7121 Standard Drive
  Hanover, MD 21076-1320

NASA / CR-2000-210654

Theoretical Analysis of the Electron Spiral Toroid Concept

Jean-Luc Cambier and David A. Micheletti
MSE Technology Applications, Inc., Butte, Montana

National Aeronautics and
Space Administration

Langley Research Center
Hampton, Virginia 23681-2199

Prepared for Langley Research Center
under Purchase Order L-8871

December 2000

Acknowledgments

Work was conducted through the U.S. Department of Energy–National Energy Technology Laboratory at the Western Environmental Technology Office under DOE Contract Number DE-AC22-96EW96405.

Available from:

NASA Center for AeroSpace Information (CASI)
7121 Standard Drive
Hanover, MD 21076-1320
(301) 621-0390

National Technical Information Service (NTIS)
5285 Port Royal Road
Springfield, VA 22161-2171
(703) 605-6000

Contents

Section Page

Figures iv
Tables iv

Executive Summary 1
1. Introduction 2
2. Fundamental Dynamics 3
3. The EST Configuration 5
4. Stability Problems 11
5. The EPS Theoretical Model 14
6. Scaling Properties 18
7. Energy Storage and Lifetime 21
8. Experimental Observations 30
9. Conclusions 32
10. References 35

Figures

Page

1: Schematic of EST plasma 2
2: Schematic of coordinate transformation. The z-direction is out of plane. The toroid is approximated by an infinitely long cylinder 3
3: Numerical solution of Equations (21) and (24) (electrons only) for the choice of parameters: $\alpha = 1.6$, $\hat{f} = 1.02$, $r_b / r_1 = 1.01$ (Case # 1 in Table 1) 8
4: Numerical solution (electrons only) for the choice of parameters: $\alpha = 10^3$, $\hat{f} - 1 = 10^{-4}$, $r_b / r_1 = 1.01$ (see Case #2 in Table 1) 8
5: Normalized velocity for Case #3 (compare with Figure 4 of [1]) 9
6: Normalized cyclotron frequency for Case #3 (compare with Figure 5 of [1]) 9
7: Normalized velocity for Case #4 of Table 1 (symbols are plotted every 5 grid points) 10
8: Normalized cyclotron frequency for Case #4 of Table 1 (symbols plotted for every 5 grid points) 10
9: Comparison between the two terms of Equation (30) determining extent of physical solution for the ion velocity. Results for Case #3 of Table 1 12
10: Comparison between the two terms of Equation (30) determining extent of physical solution for the ion velocity. Results for Case #4 of Table 1 12
11: Scaling relationship between coupling parameter α and charge parameter $\hat{f} - 1$ for constant magnetic field 19
12: Scaling relationship for constant electron energy 19
13: Scaling of electron energy versus shell thickness 20
14: Scaling of magnetic field with size ratio. Both data and approximate fit shown 20
15: Schematic of kinetics at the EST interface 28

Tables

1: List of cases studied by Chen in [1] 7
2: Comparison of our numerical results with those of Chen in [1] 7
3: EST parameters listed in [2] 21
4: Typical structural parameters satisfying energetic values in Table 3 22

Executive Summary

This report describes the analysis by MSE Technology Applications, Inc. (MSE) of the Electron Spiral Toroid (EST) concept being developed by Electron Power Systems Inc. (EPS). This analysis was conducted for the National Aeronautics and Space Administration's Langley Research Center (NASA-LaRC). The EST is described by EPS as a plasma shell of toroidal shape, in which electrons are in orbits around the toroidal axis. The current produced by the electron motion generates a toroidal magnetic field, which is confined within the torus shell. It is claimed that this plasma structure is very stable and can store vast amounts of energy, primarily as a magnetic field. The most detailed description is found in a theoretical study of the EST concept performed by the Massachusetts Institute of Technology (MIT) and published by EPS, herein listed as reference [1]. EPS also recently published the Phase I report for a NASA Institute of Advanced Concepts (NIAC) award, in which some of the specific claims about lifetime and energy density storage were made, denoted herein as reference [2]. The present analysis was originally based on these and another document describing the EST concept, which was also published by EPS [3]. However, dissemination of an early draft of this report led to a further exchange of information between MSE and EPS [4]; the release of two new documents [5,6]; and multiple revisions of the model by EPS. Reference [5] is actually a revised version of [3], and the second document [6] is an experimental report for the Defense Special Weapons Agency (DSWA). The analysis of this additional material is included in the final version of this report.

Following the original description of the EST, the present analysis is mainly based on the cold-fluid equations for the plasma shell coupled to the self-generated magnetic field. The dynamical equations of the cold electron fluid, as well as the numerical solutions, are found to match those presented in [1]. However, these equations only represent an incomplete subset of the plasma dynamics, since the ion motion was ignored. It is easily seen that the ion fluid is unstable, due to the repulsing electrostatic field required for electron confinement. A detailed analysis with the numerical procedure confirmed these results. The EST concept requires an excess of positive charges, and the potential well thus created is responsible for confining the electrons as well as the magnetic field stored within the torus. Although various scenarios for ion confinement were then suggested [4,8] by EPS and MIT, none of them is plausible. In fact, it is demonstrated in this report that this problem is fundamental and cannot be solved within the context of the proposed EST configuration. Several problems were also found with the results presented in [2] regarding the physical characteristics of a high-energy EST, which were found to be inconsistent with the scaling properties of the numerical solutions. The rates of energy losses through collisions and cyclotron emission were also examined and found to be in error by several orders of magnitude. Furthermore, the analysis by EPS of the experimental data [6] does not provide proof of an EST, as defined in [1].

It is demonstrated in this report that the claims of absolute stability and large energy storage capacities of the EST concept have not been substantiated. However, there is undeniable experimental evidence of some type of plasma structures whose properties and characteristics still remain to be determined and which could potentially have applications for space propulsion. However, more realistic theoretical models must first be developed to explain their existence and properties before applications of interest to NASA can be assessed and developed.

1. Introduction

This report describes the analysis by MSE Technology Applications, Inc. (MSE) of the Electron Spiral Toroid (EST) concept being developed by Electron Power Systems Inc. (EPS). This analysis was conducted for the National Aeronautics and Space Administration's Langley Research Center (NASA-LaRC). The company received a Phase I award from the NASA Institute for Advanced Concepts (NIAC) – grant number 07600-013. The information regarding the EST concept is somewhat sketchy, since there are no peer-reviewed publications. Our first analysis of the concept was completed in November 1999, and was based on the limited literature available at the time; primarily a theoretical description of the concept by C. Chen [1], the NIAC Phase I report [2], as well as an EPS document describing other aspects of the concept [3]. After the release of an earlier version of this report and a discussion with EPS investigators [4], further information was made available [5,6] and subsequently reviewed. Finally, a meeting took place with EPS and the Massachusetts Institute of Technology (MTI) [7] during which the latest, nonpublished information [8,9] was made available. Note also that references [3,5,8] are different versions of a similar document; the revisions were made following the results of the present analysis.

In the original "published" documents [1-8], it is claimed that a "stable" plasma, capable of storing vast amounts of energy, can be created without the need for external confinement (i.e., "free" ESTs). There is no exact definition of "stable", but indications from the available literature [2,3] suggest lifetimes of the order of *years*. Since plasmas in laboratories are notoriously short-lived entities, this claim is quite spectacular. Other claims are similar in scope. For example, the EST specific energies could be of the order of 6×10^{16} J/kg. By comparison, combustion of 1 kg of hydrogen with oxygen would generate 1.2×10^{8} J, which is equivalent to the liberation of approximately 1.25 eV/atom. To reach the claimed level of specific energy, each atom would have to be able to store 650 MeV of energy (approximately 60% of the rest-mass of the proton itself)! To date, only antimatter is known to have this level of energy density. The stored energy would primarily be in the form of a confined magnetic field, of the order of 16,000 Tesla. This would lead to an internal pressure of 1 *billion* atmospheres, yet no external confinement method is mentioned.

The plasma in the EST is basically contained within a toroidal shell, with the electrons at high velocity in the poloidal direction (i.e., in orbit around the centerline of the torus). The electron motion generates a magnetic field along the toroidal direction, which forms the greater circle of radius R_T . A schematic of the concept is shown in Figure 1 below (taken from [2]).

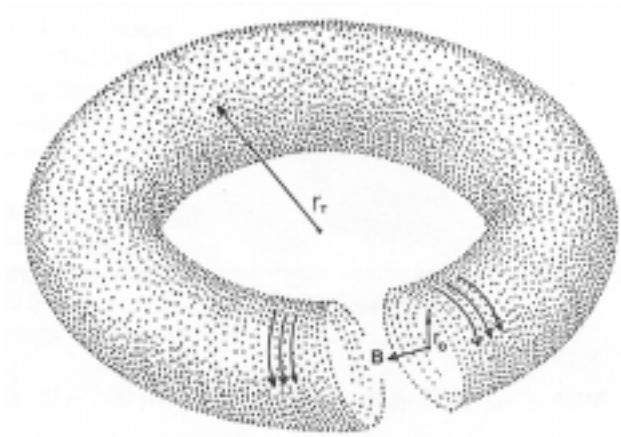

Figure 1: Schematic of EST plasma.

The plasma is assumed to be strongly coupled. The analysis of plasma dynamics in [1] is based only on the cold-fluid model, which is certainly valid for strongly coupled plasmas. It is sufficient to say that thermal effects are assumed to be nonexistent or negligible, and therefore, they are not considered in [1] or in the present analysis.

2. Fundamental Dynamics

The toroid of inner radius r_b and outer radius R_T, shown in Figure 1, can be approximated by an infinitely long cylinder. The examination of the stability properties of the toroid can then be reduced to a two-dimensional problem. As described in [1], the plasma is considered to be within a toroidal shell, between the boundary radius r_b and an inner boundary r_1. The plasma is therefore contained in a cylindrical shell. This configuration is identical to the one described in [1]. Consider also the transformation from an orthogonal coordinate system ($\hat{x}, \hat{y}, \hat{z}$) into a cylindrical coordinate system[†] ($\hat{r}, \hat{\varphi}, \hat{z}$), as shown in Figure 2. The associated transformation matrix R_φ describes a rotation by an angle φ, such that:

$$\begin{pmatrix} u_x \\ u_y \end{pmatrix} = R_\varphi \begin{pmatrix} u_r \\ u_\varphi \end{pmatrix} = \begin{pmatrix} \cos\varphi & -\sin\varphi \\ \sin\varphi & \cos\varphi \end{pmatrix} \begin{pmatrix} u_r \\ u_\varphi \end{pmatrix}, \tag{1}$$

$$\begin{pmatrix} u_r \\ u_\varphi \end{pmatrix} = R_\varphi^{-1} \begin{pmatrix} u_x \\ u_y \end{pmatrix} = -\begin{pmatrix} \cos\varphi & \sin\varphi \\ \sin\varphi & \cos\varphi \end{pmatrix} \begin{pmatrix} u_x \\ u_y \end{pmatrix}, \tag{2}$$

and

$$\begin{pmatrix} \partial_x \\ \partial_y \end{pmatrix} = R_\varphi \begin{pmatrix} \partial_r \\ r^{-1}\partial_\varphi \end{pmatrix} \tag{3}$$

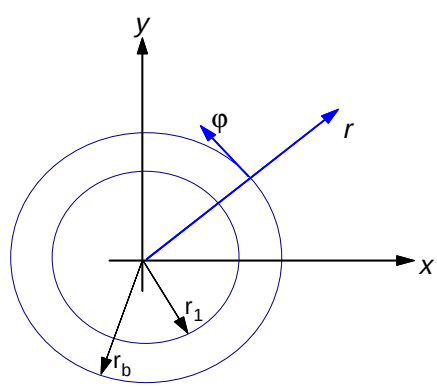

Figure 2: Schematic of coordinate transformation. The z-direction is out of plane. The toroid is approximated by an infinitely long cylinder.

The equation of motion for a cold, incompressible plasma fluid is:

$$\frac{\partial \vec{u}_\alpha}{\partial t} + \left(\vec{u}_\alpha \cdot \vec{\nabla}\right)\vec{u}_\alpha = \frac{Z_\alpha e_\alpha}{m_\alpha}(\vec{E} + \vec{u}_\alpha \times \vec{B}) \tag{4}$$

[†] In the torus, the $\hat{z}$ direction becomes $\hat{\theta}$, the toroidal direction.

where $\alpha = e, i$ is the index for the plasma component (electrons and ions). The dynamical Equation (4) can then be expressed in the cylindrical coordinate system, using the fact that the magnetic field has a component in the $\hat{z}$ direction only:

$$\partial_t u_r + u_r \partial_r u_r - \frac{u_\varphi^2}{r} = \frac{Z_\alpha e}{m_\alpha}(E_r + u_\varphi B_z) \tag{5-a}$$

$$\partial_t u_\varphi + u_r \partial_r u_\varphi + \frac{u_r u_\varphi}{r} = \frac{Z_\alpha e}{m_\alpha}(E_\varphi - u_r B_z) \tag{5-b}$$

Since one is interested in steady equilibrium conditions, the time-derivatives and the radial velocity are assumed to be identically zero. The equilibrium configuration being symmetric, we also have $E_\varphi \equiv 0$. The only velocity is in the $\hat{\varphi}$ direction, the only electric field is in the $\hat{r}$ direction only, and the magnetic field is in the $\hat{z}$ direction. Therefore, one can drop the spatial index for these quantities. Assuming a single species of ions of mass m_i, we then have:

$$\begin{aligned} \frac{u_e^2}{r} &= \frac{e}{m_e}(E + u_e B) \\ \frac{u_i^2}{r} &= -\frac{Z_i e}{m_i}(E + u_i B) \end{aligned} \tag{6}$$

The electric field is given by Poisson's equation, i.e.:

$$\frac{1}{r}\partial_r (rE) = \frac{e}{\varepsilon_o}\left(Z_i n_i(r) - n_e(r)\right) \tag{7}$$

At this stage, it is useful to introduce density scales $\overline{n}_e, \overline{n}_i$ and bring all the spatial dependence into normalized functions $f_e(r), f_i(r)$, such that:

$$n_e(r) = \overline{n}_e f_e(r) \quad ; \quad Z_i n_i(r) = \overline{n}_i f_i(r) \quad \text{and} \quad \Delta f(r) = f_i(r) - f_e(r) \tag{8}$$

A spatial scale is also introduced as the minor radius of the toroid, r_b and a normalized radial variable defined as:

$$\rho = \frac{r}{r_b} \quad ; \quad 0 \le \rho \le 1 \tag{9}$$

Introducing also the plasma frequencies ω_{pe}, ω_{pi}:

$$\omega_{pe}^2 = \frac{e^2 \overline{n}_e}{m_e \varepsilon_o} \quad ; \quad \omega_{pi}^2 = \frac{Z_i e^2 \overline{n}_i}{m_i \varepsilon_o} \tag{9}$$

Poisson's equation becomes:

$$\frac{eE}{m}(\rho) = \frac{\omega_{pe}^2 r_b^2}{r} \underbrace{\left[\int_0^\rho d\rho' \rho' \Delta f(\rho') \right]}_{\Phi(\rho)} \tag{10}$$

The solutions of the equations of motion then become:

$$\begin{aligned} u_e(\rho) &= \frac{r}{2}\left[\omega_{ce} \pm \sqrt{\omega_{ce}^2 + 4\omega_{pe}^2 \Phi(\rho)/\rho^2} \right] \\ u_i(\rho) &= \frac{r}{2}\left[-\omega_{ci} \pm \sqrt{\omega_{ci}^2 - 4\omega_{pi}^2 \Phi(\rho)/\rho^2} \right] \end{aligned} \tag{11}$$

where the definitions of the cyclotron frequencies have been used:

$$\omega_{ce} = \frac{eB}{m} \quad ; \quad \omega_{ci} = \delta\omega_{ce} \quad \text{with} \quad \delta = \frac{Z_i m_e}{m_i} \tag{12}$$

Finally, the magnetic field is given by Ampere's law:

$$\partial_r B = -e\mu_o\left(\bar{n}_i f_i u_i - \bar{n}_e f_e u_e\right) \tag{13}$$

Assuming that the plasma is nearly neutral, one can set $\bar{n}_i \equiv \bar{n}_e$, with any space-charge effects included in the distribution functions f_i, f_e. In that case, the evolution of the magnetic field becomes:

$$\partial_r \omega_{ce} = -\frac{\omega_{pe}^2}{c^2}\left(f_i u_i - f_e u_e\right) \tag{14}$$

Equations (10),(11) and (14), combined with the definition (12), form a closed system and can thereby be solved.

3. The EST Configuration

According to ref. [1], the EST is characterized by an electron density function of the form:

$$f_e(\rho) = \begin{cases} r_1 / r & \text{if } r_1 \le r \le r_b \\ 0 & \text{otherwise} \end{cases} \tag{15}$$

The ions form a background density with the same spatial dependence as the electrons, albeit with a slight relative excess $\hat{f}$, such that:

$$f_i(\rho) = \hat{f}\ f_e(\rho) \tag{16}$$

In that case,

$$\Phi(\rho) = \int_{r_1/r_b}^{\rho} d\rho' \rho' \Delta f(\rho') = \frac{r_1}{r_b}(\hat{f}-1)(\rho - \frac{r_1}{r_b}) \tag{17}$$

and

$$\frac{\Phi(\rho)}{\rho^2} = \left(\hat{f}-1\right)\frac{r_1}{r}\left(1 - \frac{r_1}{r}\right) \tag{18}$$

Although there is no other explicit information regarding the ions in the EST model, it is assumed that they provide a *fixed* background since the ion equation of motion is not being considered in [1]. It should also be pointed out that there is a somewhat confusing statement in [2], where the parameters of a large-scale EST are listed (page 11 of ref. [2]). Although the total charge is 186 coulombs, the system is called "charge-neutral". Even though the relative deviations from neutrality would appear small[†], the densities considered in these intense EST configurations lead to a large amount of electrostatic energy. In fact, it is precisely this electrostatic charge that is responsible for containment of the plasma and storage of the intense (16,000 Tesla!) magnetic field. At sufficiently large distances from the EST, the electric field given by the EST can be approximated by the zeroth-order term in the multipolar expansion:

$$E \approx \frac{Q}{4\pi\varepsilon_o R^2} \tag{19}$$

[†] For example, the last theoretical case considered in [1] (page 16) uses a deviation $\hat{f} - 1 = 5\times10^{-7}$.

which (for the 186 Coulombs quoted in [2]) gives a field of $E \approx 1.7 \times 10^{12}\ V/m$ at 1 m distance. It is not known how the developers of the EST intended to prevent electrical discharges from spontaneously occurring between the EST and its surroundings, given this level of field intensity.

Nevertheless, the theoretical analysis of the EST concept, as described in [1], can be continued. It is useful to introduce further normalization parameters, such that:

$$v_e = \frac{u_e}{\omega_{pe} r_1} \quad ; \quad v_i = \frac{u_i}{\omega_{pe} r_1} \tag{20-a}$$

and

$$\hat{\Omega}_{ce} = \frac{\omega_{ce}}{\omega_{pe}} \quad ; \quad \hat{\Omega}_{ci} = \frac{\omega_{ci}}{\omega_{pe}} \tag{20-b}$$

Instead of normalizing the distance to the boundary of the toroid (Equation (9)), one can scale the distance with respect to the inner radius of the electron shell, as in [1]: $\rho = r / r_1$. In that case, the electron velocity is given by:

$$v_e = \frac{\rho}{2}\left[\hat{\Omega}_{ce} \pm \sqrt{\Omega_{ce}^2 + 4(\hat{f} - 1)\tfrac{1}{\rho}(1 - \tfrac{1}{\rho})}\right] \tag{21}$$

Introducing the coupling parameter:

$$\alpha = \frac{\omega_{pe}^2 r_1^2}{c^2} \tag{22}$$

and since the ions are fixed, the equation for the magnetic field can simply be written as:

$$\frac{\partial \hat{\Omega}_{ce}}{\partial \rho} = \alpha \frac{v_e}{\rho} \tag{23}$$

and therefore:

$$\frac{\partial \hat{\Omega}_{ce}}{\partial \rho} = \frac{\alpha}{2}\left[\hat{\Omega}_{ce} \pm \sqrt{\Omega_{ce}^2 + 4(\hat{f} - 1)\tfrac{1}{\rho}(1 - \tfrac{1}{\rho})}\right] \tag{24}$$

Equations (21) and (24) describe the evolution of the system and are completely identical to Equations (23) and (24) or ref. [1].

Therefore, the dynamical system of the EST (as described in [1]) has been recovered. This is a nonlinear system, which requires a numerical integration procedure. Therefore, a simple numerical procedure for the solution of the system (21, 24) was written, and numerical solutions were obtained for the same parameters as those given in [1]. For example, the normalized solution for $\alpha = 1.6$, $\hat{f} = 1.02$, and $r_b / r_1 = 1.01$ is shown in Figure 3. Note that the boundary radius r_b used here is equivalent to the r_{b2} radius used in [1]. The solution presented in Figure 3 is completely identical to the corresponding Figure 2 of ref. [1]. All the cases computed in [1] are listed in Table 1 and have been recomputed with our numerical integration code. These solutions are shown in Figures 3 through 8 and are identical with the results presented in [1]. However, there are no figures corresponding to the last case (#4) in [1]. Special attention has been given to the solution accuracy, and the current numerical scheme uses a stretched grid near the edges of the plasma shell, such that a smooth solution is guaranteed in that region.

Using the parameters listed in Table 1, the physical solutions can be obtained from the normalized numerical solutions. Of special interest are the peak electron velocity (at the outer edge of the toroidal shell), the peak magnetic field (at the inner edge of the shell), and the total

number of electrons (and ions) in the shell. The latter can be approximately obtained from the electron density and the volume of the toroidal shell, neglecting the variation of the density ($\bar{n}_e r_1/r$) within the thin shell ($r_{b2}-r_1 \ll r_1$). Since r_1 and α are given, the plasma frequency can be obtained from Equation (22) and the electron density from the definition of the plasma frequency (9). The volume of a thin torus ($R_T \gg r_b$) is approximately given by:

$$Vol_T \approx 2\pi^2 R_T r_b^2 \tag{25}$$

and since the plasma is contained within the shell delimited by r_1, r_{b2}, its volume is:

$$Vol_p \approx 2\pi^2 R_T \left(r_{b2}^2 - r_1^2\right) \tag{26}$$

And therefore, we approximately have:

$$N_e = Vol_p \left(\frac{\alpha c^2}{r_1^2} \frac{m_e \varepsilon_o}{e^2} \right)^{1/2} \tag{27}$$

A more accurate value of the total number of electrons N_e can be obtained by integrating the density profile during the numerical integration. This is accomplished in MSE's code.

The results for all cases considered by Chen in [1] are shown in Table 2. Note that the velocities and magnetic fields can be either positive or negative, depending on the sign of the solution taken in Equations (21) and (24). Only the absolute magnitudes are listed in Table 2. With a few exceptions, the current results compare very well with Chen's. The discrepancy in N_e for the first two cases is obviously an accounting error in [1]. Our results are consistent with the approximation (27). Another discrepancy is in the field value for Case #4. Since the normalized solution was not shown in [1], it is difficult to assess whether the error lies in Chen's numerical solution or in the rescaling. Since the electron velocities agree very well for this case and the numerical accuracy is better for the field than for the velocity profile (the velocity gradient becomes very large near the boundary at large α, thus necessitating a highly stretched grid), one can reasonably assume that Chen's numerical solution is also accurate. Therefore, it is assumed that there is a simple scaling error in [1]. As will be discussed below, our values of the magnetic field are seen to obey strict scaling laws, thus adding validity to the current results.

Case #	α	*f*-1	r_2/r_1	r_1 (m)	R_T (m)
1	1.6	2×10^{-2}	1.01	4.95×10^{-4}	2.5×10^{-3}
2	10^3	1×10^{-4}	1.01	1.00×10^{-2}	0.10
3	2×10^4	4×10^{-5}	1.05	1.50×10^{-2}	0.15
4	4×10^6	5×10^{-7}	1.05	1.50×10^{-2}	0.15

Table 1: List of cases studied by Chen in [1].

Case	$U_e(r_2)$ (m/s)		$B_\theta(r_1)$ (T)		N_e	
	Chen	current	Chen	current	Chen	current
1	5.37×10^6	5.39×10^6	6.60×10^{-4}	6.64×10^{-4}	2.24×10^{10}	4.50×10^{10} †
2	9.49×10^6	9.48×10^6	1.49×10^{-2}	1.48×10^{-2}	5.61×10^{14}	1.11×10^{15} †
3	6.00×10^7	5.99×10^7	0.69	0.70	1.68×10^{17}	1.67×10^{17}
4	9.51×10^7	9.48×10^7	21.2	15.58 ‡	3.36×10^{19}	3.34×10^{19}

Table 2: Comparison of our numerical results with those of Chen in [1]†.

† It would appear that the total number of particles in [1] have been erroneously divided by 2 in these two cases. The correct number can easily be obtained from the torus volume and the electron plasma frequency, using Equation (22).

‡ Notice the discrepancy in magnetic field in this case, while the velocity is in good agreement.

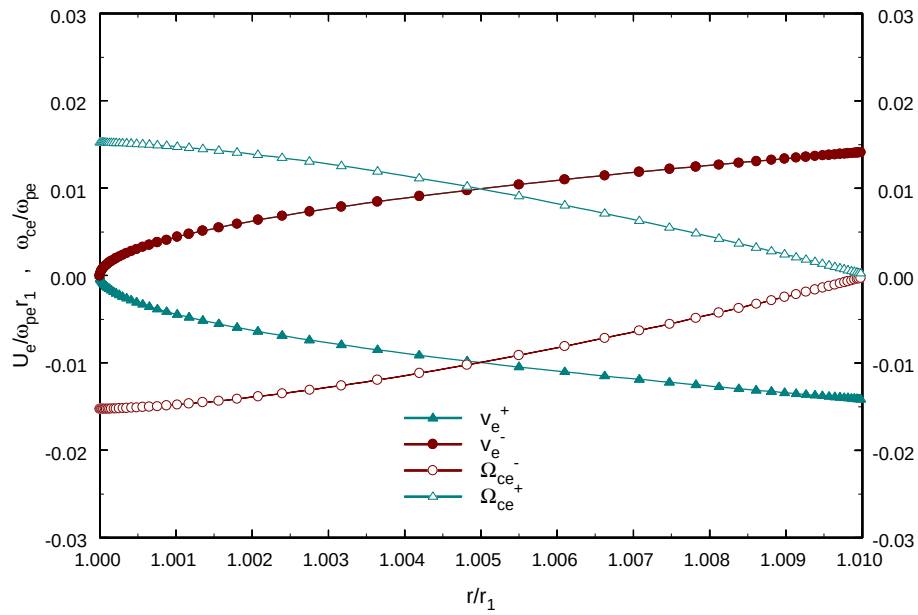

Figure 3: Numerical solution of Equations (21) and (24) (electrons only) for the choice of parameters: α =1.6, $\hat{f}$=1.02, r_b/r_1=1.01 (Case # 1 in Table 1).

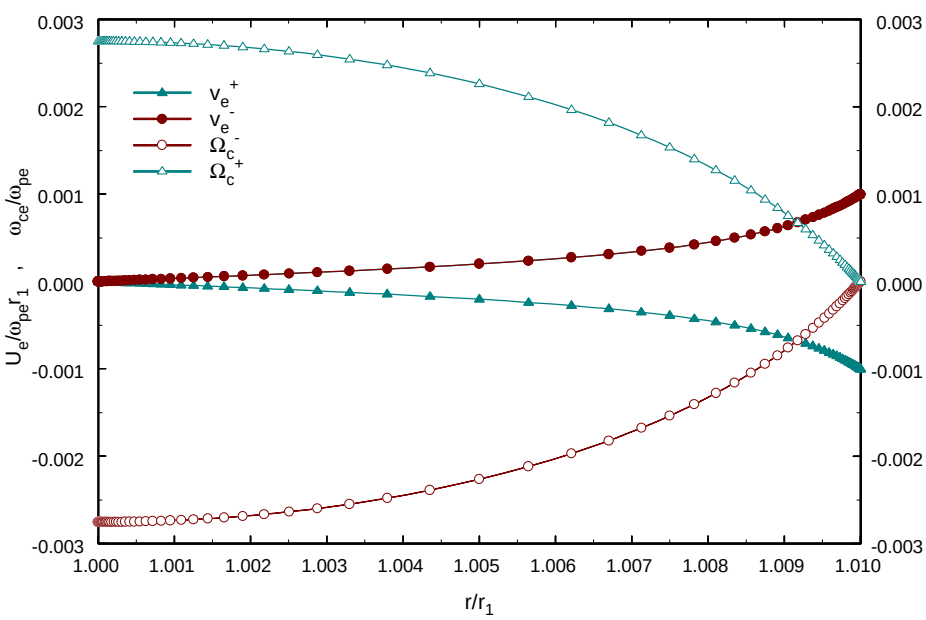

Figure 4: Numerical solution (electrons only) for the choice of parameters: α =10^3, $\hat{f}-1$=10^{-4}, r_b/r_1=1.01 (see Case #2 in Table 1).

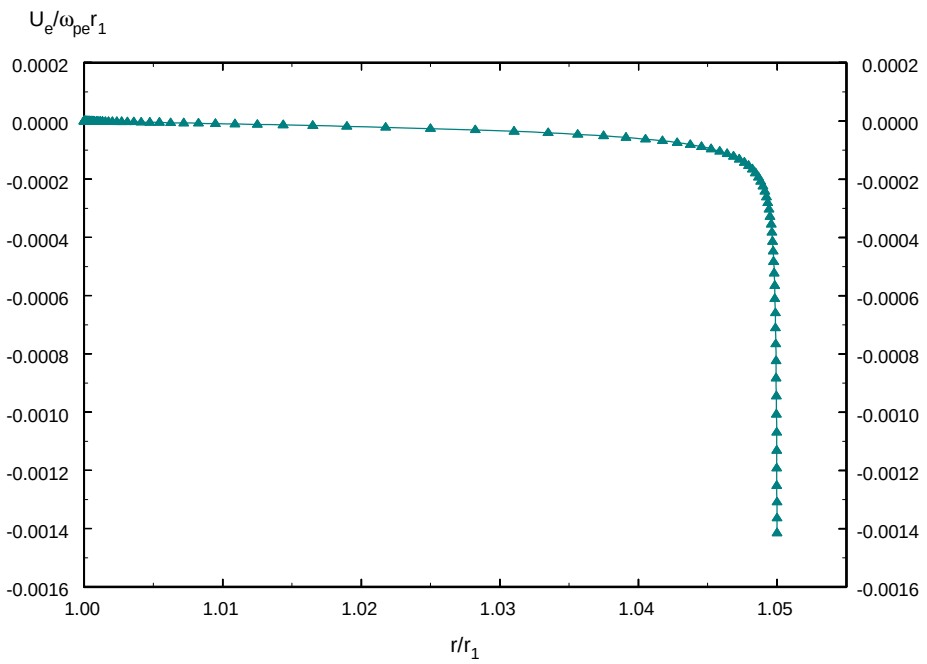

Figure 5: Normalized velocity for Case #3 (compare with Figure 4 of [1]).

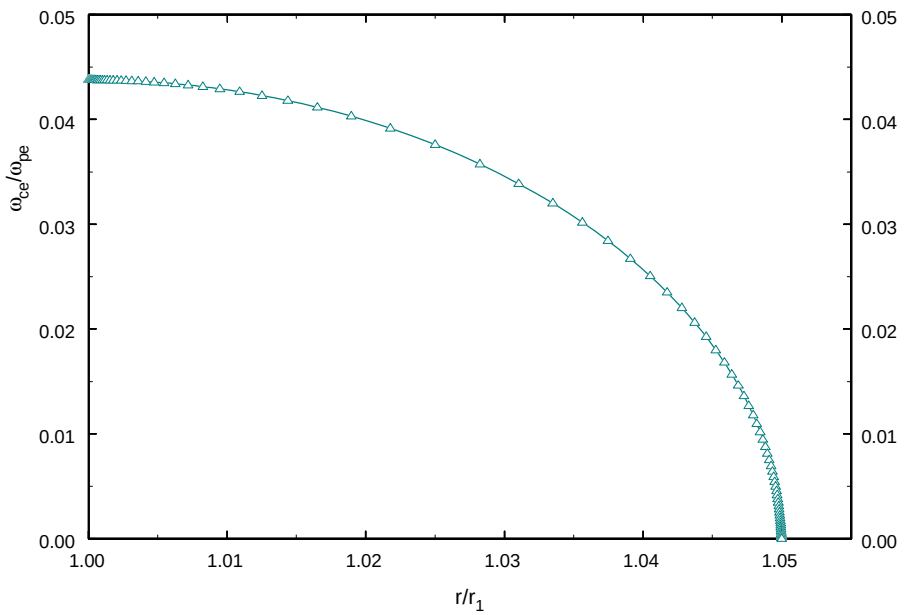

Figure 6: Normalized cyclotron frequency for Case #3 (compare with Figure 5 of [1]).

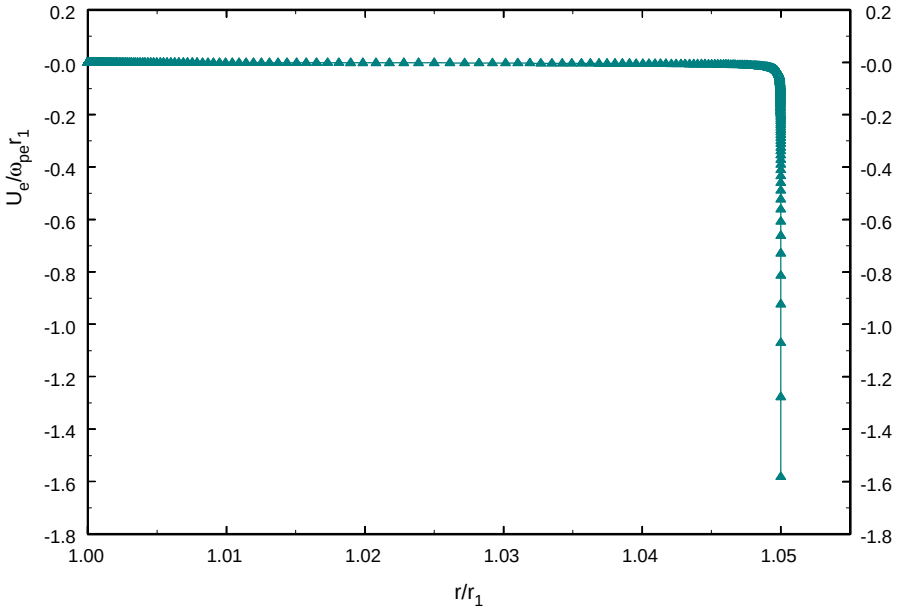

Figure 7: Normalized velocity for Case #4 of Table 1 (symbols are plotted every 5 grid points).

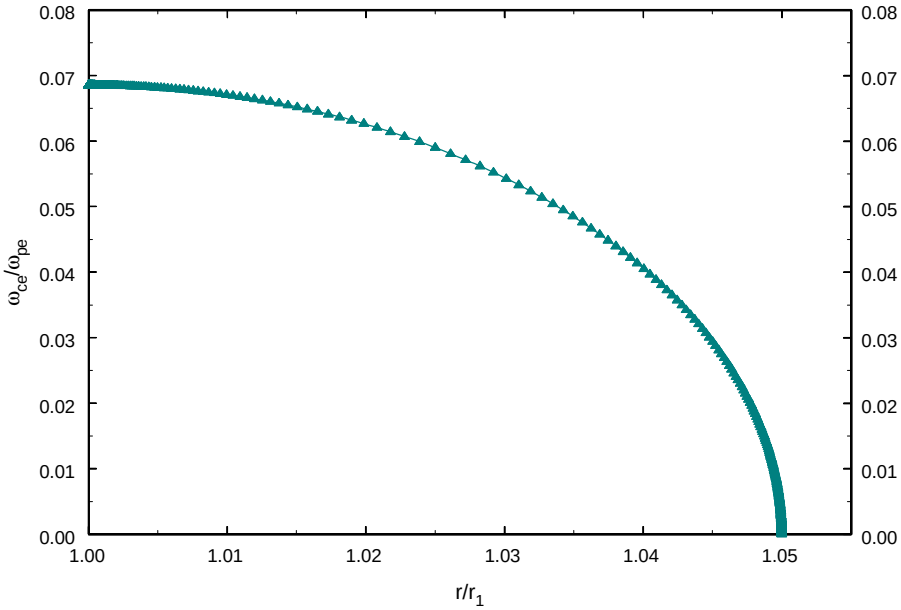

Figure 8: Normalized cyclotron frequency for Case #4 of Table 1 (symbols plotted for every 5 grid points).

4. Stability Problems

Both the dynamical equations and the numerical solutions of ref. [1] have been recovered, which would seem to bring some validity to the EST concept. However, it is crucial to examine the dynamical behavior of the *complete* system of equations *including the ions*! A key assumption barely mentioned in [1] is that the ions form a fixed background. However, since the magnetic field vanishes at the boundary of the toroid, there is no confining force being applied to the ion fluid near the surface. Since the toroid is also positively charged (the electrostatic force provides the confining force for the *electrons*), there is a strong repulsion pushing the ions outward. Therefore, there is no mechanism for keeping the ions inside the toroid. They would very rapidly "evaporate", thereby leaving the toroid absolutely charge-neutral. This process would also eliminate the confining force for the electrons, and the whole toroid would then rapidly expand, unable to contain the magnetic pressure. To look at the ion dynamics, consider Equations (5-a,b). For no initial azimuthal (i.e., poloidal) velocity ($u_{i\varphi} \equiv 0$), and since $E_r > 0$ ($\hat{f} > 1$ for electron confinement), Equation (5-a) clearly yields $\partial_t u_r > 0$, and the ion gas is rapidly expanding. The fixed ion background assumption is therefore *completely invalid* for ion-motion time scales.

One could then argue that a stable solution could still be achieved, but with the ions in motion. It is clear that as ions gain a radial velocity, the Lorentz force will also act to provide them with an azimuthal velocity (see Equation (5-b)). In that case, one must examine the stable solution of the ion fluid with an azimuthal velocity. The ion solution has already been described in Equation (11). Using the same normalization (20-a,b), one obtains (for the same density distribution):

$$v_i = \frac{\rho}{2}\left[-\hat{\Omega}_{ci} \pm \sqrt{\Omega_{ci}^2 - 4(\hat{f}-1)\tfrac{1}{\rho}(1-\tfrac{1}{\rho})}\right] \tag{28}$$

Using (12), this can also be written as:

$$v_i = \delta\,\frac{\rho}{2}\left[-\hat{\Omega}_{ce} \pm \sqrt{\Omega_{ce}^2 - \tfrac{4}{\delta}(\hat{f}-1)\tfrac{1}{\rho}(1-\tfrac{1}{\rho})}\right] \tag{29}$$

A stable solution is possible if the discriminant remains positive, i.e., if:

$$\Delta_i = \hat{\Omega}_{ce}^2 - \Psi^2 \geq 0 \tag{30}$$

with

$$\Psi^2 = \frac{4}{\delta}\left(\hat{f}-1\right)\frac{r_1}{r}\left(1-\frac{r_1}{r}\right) \tag{31}$$

Obviously, since the field vanishes at $r = r_{b2}$, $\hat{\Omega}_{ce} = 0$ and the condition cannot be satisfied. In fact, there will be a region of finite extent near the outer boundary, where this condition cannot be satisfied. The size of this region depends on the parameters α and $\hat{f}-1$. Figures 9 and 10 show plots of both $\hat{\Omega}_{ce}^2$ and Ψ^2 for Cases #3 and #4 of Table 1. The allowed region where a physical solution can be found for the ions is determined by the distance between the origin ($r = r_1$) and the point at which the two curves cross each other. For Case #3 (Figure 9), it appears that most of the plasma in the shell would be unstable to ion "evaporation". For Case #4, this region is much smaller. One could argue that for the right choice of parameters, the unstable region would be reduced to a "skin". However, this does not solve the problem since the ions would always be emitted from the surface of the EST. As the relative charge ratio $\hat{f}$ drops, the electrostatic confining force would also drop, and the torus would rapidly expand under the pressure of its own magnetic field. As the EST surface increases during expansion, so would the rate of ion loss.

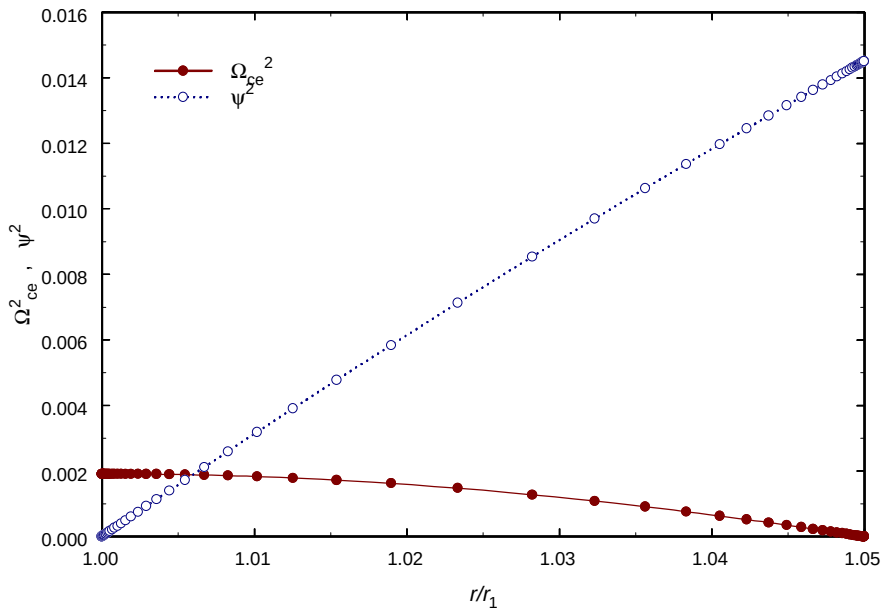

Figure 9: Comparison between the two terms of Equation (30) determining extent of physical solution for the ion velocity. Results for Case #3 of Table 1.

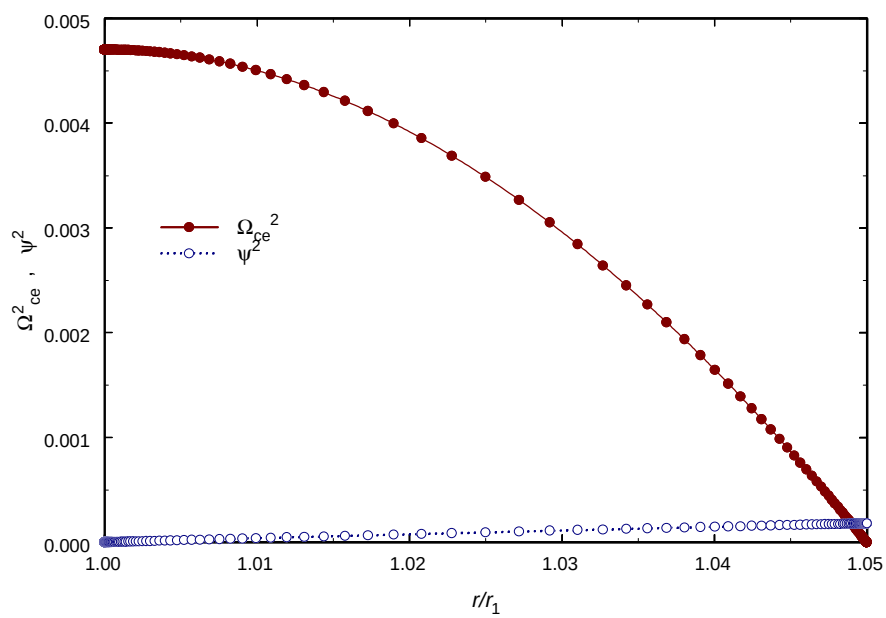

Figure 10: Comparison between the two terms of Equation (30) determining extent of physical solution for the ion velocity. Results for Case #4 of Table 1.

The process is self-accelerating and would eventually lead to the explosive liberation of the stored energy. However, there are still further problems that prevent a stable solution. As the Δ_i term becomes positive and a physical solution for the ions can be found, the dynamics are no longer governed by Equations (21) and (24). In fact, the full expression for the current must be used (including the ion velocity) and the evolution of the magnetic field is now given by Equation (14), or its normalized equivalent. Solving for the complete system, it is found that no physical solution can be obtained. Detailed examination of the results reveals that the problem has nothing to do with numerical errors. It is first necessary to point out an important aspect of the dynamics of the problem. There are two possible solutions for the electron velocity, depending on the sign chosen in Equation (21). If the "+" sign is chosen (and $v_e^+ > 0$), the field takes on negative values ($\hat{\Omega}_{ce}^+ < 0$). If the "-" sign is chosen (and $v_e^- < 0$), the field is positive ($\hat{\Omega}_{ce}^- > 0$). This can easily be seen on Figures 3 and 4. In either case, the dynamics are such that the absolute value of the electron velocity is given by a difference between two terms: $\hat{\Omega}_{ce}$ and the square root term of Equation (21). Therefore, using the definition (31), one can write:

$$v_e = -\frac{\rho}{2}\hat{\Omega}_{ce}\left[1-\sqrt{1+\frac{\delta\,\Psi^2}{\hat{\Omega}_{ce}^2}}\right] \tag{32}$$

However, at the crossover point where the ion fluid can have a physical solution, $\hat{\Omega}_{ce}^2 \approx \Psi^2$, and therefore:

$$v_e \approx -\frac{\rho}{2}\hat{\Omega}_{ce}\left[1-\sqrt{1+\delta}\,\right] \approx \delta\,\frac{\rho}{4}\hat{\Omega}_{ce} \tag{33}$$

in that region.

On the other hand, the ion velocity is approximately:

$$v_i \approx -\delta\,\frac{\rho}{2}\hat{\Omega}_{ce} \tag{34}$$

since the square-root term in Equation (29) vanishes at the crossover point. Therefore, at the crossover, the ion velocity is approximately *twice* the magnitude of the electron velocity and with the *opposite* sign. The rate of evolution of the magnetic field immediately changes sign, and the magnitude of the field starts *decreasing* as one moves towards the inner boundary. This also implies that the discriminant Δ_i given in Equation (30) immediately ceases to be positive, and the ion fluid has no physical solution. This behavior is exactly confirmed by a careful examination of the numerical integration procedure as one attempts to find a solution that includes the ion fluid. Therefore, even if the parameters are chosen to concentrate the dynamics near the outer edge of the shell, the *complete* dynamics reveal that *no stable solution* can be found.

It is also useful to estimate the field required to enforce a stable solution for the ion fluid. This could be estimated by requiring that $\Delta_i = 0$ at the boundary $r = r_{b2}$. For example, taking Case #3 of Table 1, one finds that there must be a magnetic field at the outer boundary $r_{b2} \approx 1.01 r_1$ on the order of: $B_{ext} \approx 0.9\,T$. This is comparable to the field stored inside the EST for this case. Therefore, even if one were to provide an external confinement field, its value would need to be of the same order as the one stored inside the toroid.

As pointed out by Chen [4], the discussion of ion stability can be avoided altogether by invoking the Virial theorem ([10], pp. 72-74), which states that a plasma cannot be self-confined. However, we believe that the examination of the dynamical equations elucidates the origins of the self-

confinement problem better than maybe simply quoting a theorem. At the same time, our analysis indicates that an externally confining field would have to be of the same order as the stored field. Although this may appear obvious from energetic considerations, the result is important because it can be generalized to any method of confinement including external mechanical pressure. The magnetic energy stored inside the torus is in direct relation with the electrostatic potential energy generated by the excess charge of the ions used to confine the electrons. In turn, to confine the ions would require an energy density (i.e., a pressure) of at least the same order of magnitude.

In the introduction of ref. [1], it is mentioned that the model is valid only for time scales short in comparison with the ion motion time scale (e.g. inverse ion plasma frequency); the problem of ion confinement is therefore not addressed. This is the only mention of this important time-scale limitation in all the provided documentation. On the other hand, several EPS documents [2,3,5,8] state that the physics of the EST were derived and verified, the EST was stable with no external field required for confinement, and there was "no known or obvious normal occurrence that will lead to instability". There can be no ambiguity in the definition of "stable plasma" since the described applications require lifetimes of many hours, certainly much greater than the ion motion time scale. For example, references [3,5] explicitly mention an EST lifetime of 10^6 hours [3,5] in a <u>vacuum</u> environment.

It is then clear that the free EST, as described in [1], cannot achieve long-term stability. Further discussions with Chen [4] confirmed that mechanical pressure of some sort is required for ion confinement. The realization of a high-energy EST in a vacuum environment is therefore completely unfeasible. In a follow-on discussion [4], EPS officials implied that the references were actually for a "partial vacuum" only. This is not a valid argument, since the term "vacuum" can be used to describe any environment where the pressure is much lower than atmospheric and therefore, negligible compared to the internal pressure (gas-dynamic or electromagnetic) of the high-energy EST. At any rate, it is extremely difficult to imagine how high-energy ESTs can be confined by a mechanical pressure many orders of magnitude smaller than the stored magnetic energy. The example described in [3,5] mentions an EST with 100 MJ of stored energy, corresponding to an energy density of approximately 10^{11} J/m^3 (i.e., a magnetic pressure of 2 million atmospheres). The example in [2] corresponds to internal magnetic pressures of 1 billion atmospheres, yet one should expect these high-energy EST configurations could be absolutely stable in near-vacuum conditions! To find a mechanism that can achieve this extraordinary feat would require dramatic changes in the fundamental laws of physics. The problem of ion confinement will be further discussed in Section 7.

5. The EPS Theoretical Model

Before discussing further the implications of the cold-fluid model, it is worth investigating another theoretical model of the EST proposed by EPS, as described in [5,8]. This is an attempt at constructing a "discrete" model using a summation over a finite number of particles. The ions and electrons reside in separate shells (the ions form the inner shell), composed of a large number of loops of radius r_o and a large number of particles along each loop. The spacing between electrons on a loop is d_e, and therefore, the number of electrons in a loop is:

$$N_{(e|loop)} = \frac{2\pi r_o}{d_e} \tag{35}$$

The number of loops in the toroid is approximately ($R_T >> r_o$):

$$N_{(loop)} = \frac{2\pi R_T}{(k_o d_e)} \tag{36}$$

where $k_o d_e$ is the spacing between loops, with $k_o \approx 1$. The total number of electrons is then:

$$N_e = N_{(e|loop)} N_{(loop)} = \frac{4\pi^2 r_o R_T}{k_o d_e^2} \tag{37}$$

Note that the EST surface area is also given by:

$$Area = 4\pi^2 r_o R_T \,. \tag{38}$$

The EPS investigators first compute the force acting on an electron in a single loop. Since the distance between electrons is given by the chord $d_e = 2r_o \sin(\delta\theta/2) \approx r_o \delta\theta$, where the angular distance is of course $\delta\theta = 2\pi / N_{(e|loop)}$, the <u>radial component</u> of the electrostatic repulsion force from all electrons in a loop is then:

$$F_e = \frac{e^2}{4\pi\varepsilon_o} 2 \sum_{n=1}^{N_{(e|loop)}/2} \frac{\sin(n\delta\theta/2)}{d_n^2} \tag{39}$$

where $d_n = 2r_o \sin(n\delta\theta/2)$. The EPS investigators then use the approximation of small angles to write the final answer as:

$$F_e \approx \frac{e^2}{4\pi\varepsilon_o r_o d_e}\left(1 + \frac{1}{2} + \frac{1}{3} + \frac{1}{4} + \ldots\right) \tag{40}$$

Strictly speaking, this is a diverging series and a potential problem for large $N_{(e|loop)}$. EPS estimates the summation to be ≈5, a rather arbitrary choice. Using this small finite value for this summation, EPS then expresses the force of repulsion due to all other electrons on the loop as:

$$F_e = C^{te} \frac{e^2}{4\pi\varepsilon_o r_o d_e} \tag{41}$$

where C is a constant. Note that this is the force acting on a single electron, and that this result is obtained in the limit of large $N_{(e|loop)}$. EPS then uses this expression in the balance of forces. However, this is a serious error for several reasons.

First, the expression for the force itself (41) is wrong, because the truncation of the summation to small numbers is invalid. The summation in (40) is logarithmically divergent, and the expression for the force should then include a term $\log(r_o / d_e)$, which is not negligible.

Second, and even more importantly, this expression does not take into account the contribution from neighboring loops. Since the distance between loops is assumed by EPS to be of the same order as the distance between electrons in a loop ($k_o d_e$, with $k_o \approx 1$), this contribution is far from negligible and is, in fact, of the same order. The correct evaluation of the force is shown later in this section, but an estimation of this contribution can be given below.

To include the electrons in neighboring shells, one can replace each electron on the loop by a tube extending in the $\hat{z}$ direction (the major radius of the toroid). This tube has a diameter d_e, and the effective density of electrons in this tube is $(\pi d_e^2 k_o d_e / 4)^{-1}$. The solution of Poisson's equation for this charge configuration yields the following field strength at a distance d' from the tube:

$$E \approx \frac{4e}{\pi\varepsilon_o} \frac{1}{k_o d_e d'} \tag{42}$$

Using this value for the radial force on an electron and summing over all tubes along the loop:

$$F_e = \frac{e^2}{\pi\varepsilon_o}\frac{8}{k_o d_e}\sum_{n=1}^{N_{(e|loop)}/2}\frac{\sin(n\delta\theta/2)}{d_n} \tag{43}$$

This time, the sum can be evaluated since the $\sin(n\delta\theta/2)$ cancel out. The summation becomes:

$$\sum_{n=1}^{N_{(e|loop)}/2}\frac{1}{2r_o} = \frac{1}{2r_o}\frac{N_{(e|loop)}}{4} = \frac{\pi}{4d_e} \tag{44}$$

The force on the electron then behaves as d_e^{-2}, not as $(r_o d_e)^{-1}$ and is therefore much larger.

The errors made by EPS are then further compounded when computing the force due to the magnetic field. This is expressed in [5,8] as:

$$F_m = ev \times B = \frac{ev\mu_o iN}{2\pi R_T} \tag{45}$$

where $i = ev_e / d_e$ is the current in a single loop, and R_T is the radius of the toroid. There is some confusion as to the nature of this field. In [5,8], the magnetic field is taken as an initiating field caused by the arc current used to create the EST. In that case, it is not clear why the arc current should also be the same as the loop current, unless all the arc current goes into the toroid. In that case, the magnetic field created by the current loop should be:

$$B = \frac{\mu_o i}{2\pi r_o} \tag{46}$$

and the toroid radius R_T should not appear in these expressions. There is also confusion about the meaning of the number N appearing in (45). This should actually be the number of loops:

$$N_{loops} = \frac{2\pi R_T}{k_o d_e} \tag{47}$$

but in fact, EPS uses the product $N = N_{loop}N_{(e|loop)}$ in Equation (45). The resulting expression in [5,8] yields the force acting on *all electrons in a loop* instead of on *each* electron. The comparison with the electrostatic forces (Equations (41) or (43)) is therefore *completely invalid.*

The proper way to evaluate these forces can now be described in the same limit of large N_e. Assume that the electrons form a cylindrical shell of thickness dr. Integrating Poisson's equation (7) for the electron component only, the electric field acting on each electron becomes:

$$E = \frac{en_e}{\varepsilon_o}dr \tag{48}$$

where n_e is of course the electron density in the shell. Using the total number of electrons (37) and the shell volume $(2\pi r_o)dr(2\pi R_T)$, one can easily arrive at the final expression:

$$E = -\frac{e}{\varepsilon_o k_o d_e^2} \quad \text{and} \quad F_e = \frac{e^2}{\varepsilon_o k_o d_e^2} \tag{49}$$

Notice that this result is independent of the assumed thickness. The field due to the ion shell can be computed in a similar fashion and added (linear superposition) to yield the total electrostatic force on an electron. The magnetic field inside the toroid is approximated by a solenoidal field:

$$B = \mu_o i\left(\frac{dN_l}{dx}\right) = \mu_o i\frac{1}{k_o d_e} \tag{50}$$

or:

$$B = \frac{\mu_o e v}{k_o d_e^2} = v_e \frac{e}{\varepsilon_o k_o d_e^2} \tag{51}$$

Note that $B_z = -B$. The magnetic force on *each electron* is then:

$$F_M = \frac{\mu_o e^2 v^2}{k_o d_e^2} = \frac{e^2}{\varepsilon_o k_o d_e^2} \frac{v^2}{c^2} \tag{52}$$

Note that the ratio of magnetic to electrostatic forces is v^2 / c^2, as expected. These expressions can now be used to evaluate the balance of forces, and the contribution of the ions can be seen to be $\hat{f}$ times the force due to the electrons (49). The balance of forces for the electrons is:

$$(\hat{f} - 1) \frac{e^2}{\varepsilon_o k_o d_e^2} = e v_e B + m_e \frac{v_e^2}{r_o} \tag{53}$$

Another application consists of examining the stability of the ion shell inside the electron toroid. By symmetry, there is no electronic contribution to the electrostatic field, and the balance of forces (F_{ion}+F_{rot}=F_{mag}) *on each ion* (if possible) reduces to the following equality:

$$\hat{f} \frac{e^2}{\varepsilon_o k_o d_i^2} + m_i \frac{v_i^2}{r_i} = e v_i B \tag{54}$$

where $d_i \approx d_e$ is the ion spacing. Let us now introduce the ion Larmor radius:

$$r_{L(i)} = \frac{m_i v_i}{eB} = \left(\frac{\varepsilon_o d_e^2}{e^2} \right) (m_i c^2) \left(\frac{v_i}{v_e} \right) \tag{55}$$

where we have again used Equation (51) for the magnetic field. The centrifugal pseudo-force in Equation (54) can now be brought into the form:

$$m_i \frac{v_i^2}{r} = \left(\frac{e^2}{\varepsilon_o k_o d_e^2} \right) \left(\frac{r_{L(i)}}{r} \right) \frac{v_i v_e}{c^2} \tag{56}$$

The balance of forces for the ions (54) then implies:

$$\hat{f} \frac{e^2}{\varepsilon_o k_o d_i^2} = \left(\frac{e^2}{\varepsilon_o k_o d_e^2} \right) \left(1 - \frac{r_{L(i)}}{r_i} \right) \frac{v_i v_e}{c^2} \tag{57}$$

Both the centrifugal and magnetic forces are of the order of $v_i v_e / c^2$ and can be neglected compared to the electrostatic force. Therefore, there is no stable physical solution for the ion shell. Of course, this was also demonstrated in Section 4.

It is also interesting to examine the consequences on a mechanical confinement scheme. Suppose that the ion stability is provided by a mechanical (gas or containment vessel) pressure. In that case, the confining force applied to *each ion* must balance the electrostatic repulsion. The balance of forces then becomes:

$$\hat{f} \frac{e^2}{\varepsilon_o k_o d_i^2} + m_i \frac{v_i^2}{r} = e v_i B + F_{(conf|ion)} \tag{58}$$

Neglecting the terms of order $v_i v_e / c^2$, one can then express the required confinement force for the entire EST:

$$F_{(conf\,|\,EST)} = F_{(conf\,|\,ion)} N_{(ion)} = \left(\frac{e^2}{\varepsilon_o k_o d_i^2} \right) \left(\hat{f}\, \frac{4\pi^2 r_o R_T}{d_e^2} \right) \tag{59}$$

where the total number of ions is $\hat{f}$ times the total number of electrons, given by Equation (37). The total confinement force can be divided by the area (38) to give the confinement pressure:

$$P_{conf} = \hat{f}\, \frac{e^2}{\varepsilon_o k_o^2 d_e^2 d_i^2} \tag{60}$$

This expression can be manipulated further. Using (51), the electron spacing can be expressed as a function of the stored magnetic field:

$$k_o d_e^2 = \mu_o \frac{e v_e}{B} \tag{61}$$

In the approximation of nearly identical spacing $d_i \approx d_e$, we therefore have:

$$\varepsilon_o k_o^2 d_i^2 d_e^2 \approx (\varepsilon_o \mu_o)\, e^2\, \frac{v_e^2}{2} \left(\frac{B^2}{2\mu_o} \right)^{-1} \tag{62}$$

The confinement pressure becomes:

$$P_{conf} = \hat{f}\, \frac{2c^2}{v_e^2} \left(\frac{B^2}{2\mu_o} \right) \tag{63}$$

We can also express the ratio of speeds as a ratio of kinetic to rest mass of the electron:

$$\frac{v_e^2}{2c^2} = \frac{E_e}{m_e c^2} \tag{64}$$

and the final expression for the confining pressure becomes:

$$P_{conf} \approx \hat{f}\, P_{mag}\, \frac{511}{E_e[keV]} \tag{65}$$

Note that $\hat{f} \approx 1$ and unless the electrons are ultrarelativistic (in which case this analysis must be modified), the required confinement pressure needs to be several times larger than the magnetic field pressure inside the torus. Therefore, even if one could envision applying a confinement force on the ions[†], the required magnitude of this force is such that the concept of energy storage (i.e., a large internal magnetic field) is completely impractical. The relationship (65) is very useful because of its generality and independence with respect to the EST dimensions.

We conclude that the theoretical model proposed by EPS is severely flawed in many aspects and does not provide a stable solution. The only correct theoretical model at this stage is the cold-fluid model, which is described in [1] and also in the present analysis. However, Chen's model is incomplete, since the ion motion has not been considered. More complex descriptions of the plasma suggested by Chen (e.g. phase-space approach) would not change the fundamental properties of the model, and would therefore not solve the problem of ion confinement. For that, a completely different physical model may be necessary.

6. Scaling Properties

Although it has been determined that the EST (as described anywhere in the literature [1-8]) is not a stable structure, there are other claims to be evaluated. It is first necessary to examine the

[†] It is not clear how EPS proposes to apply a mechanical (e.g. containment vessel or gas pressure) force to the inner shell of the ions without affecting the outer shell of the electrons. As is shown in Section 7, it is not possible to prevent collisions between electrons and other particles if put into contact.

scaling properties of the structure, which will help in the examination of the claims of [2]. The incomplete solutions, found with only the electron dynamics, are analyzed as function of the "structural" parameters α and $\hat{f}-1$. The dimensions of a large-scale EST are chosen as follows:

$$r_1 = 0.15 \text{ m}, \quad r_{b2}/r_1 = 1.05, \quad R_T = 1.5 \text{ m}$$

It is therefore a scaled-up version of Cases #3 and #4 of Table 1. A series of numerical solutions can then be obtained for various values of α and $\hat{f}-1$ and characterized as a function of the maximum magnetic field $B_{\max}$ (at the inner boundary r_1) and maximum electron kinetic energy $E_{e,\max}$ (at the outer boundary r_{b2}). The results are shown in Figure 11 for a constant maximum field, chosen to be approximately 16,000 Tesla. The results for a constant maximum electron energy (chosen to be 12.5 MeV (sic)) are shown in Figure 12.

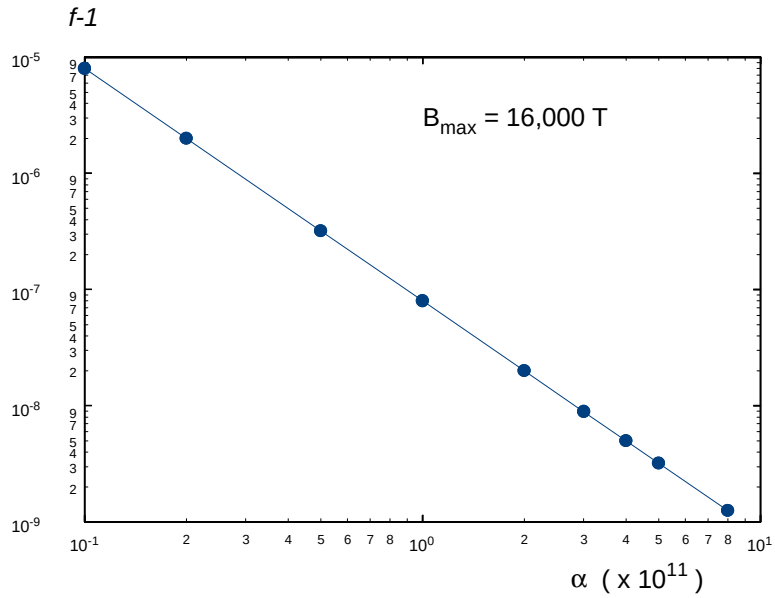

Figure 11: Scaling relationship between coupling parameter α and charge parameter $\hat{f}-1$ for constant magnetic field.

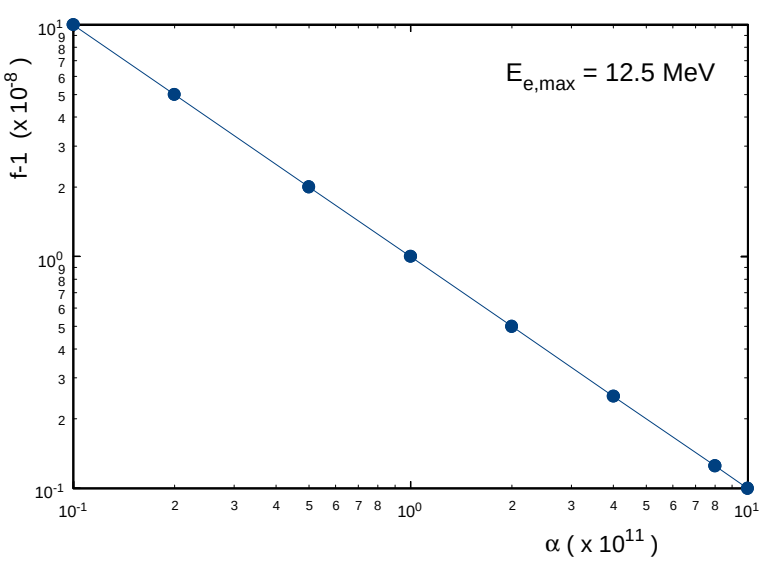

Figure 12: Scaling relationship for constant electron energy.

One should point out that this choice of electron energy is completely arbitrary and is only intended to demonstrate the obvious scaling relationship shown in Figure 12. A large electron energy allows one to cover a wide range of values of the α and $\hat{f}$ parameters. Another choice, such as the 10 keV used below, would give a line parallel to the one shown in Figure 12. The physical answers for the magnetic field and electron energy would also depend on another "structural" parameter, the relative shell thickness (i.e., the ratio r_{b2}/r_1). For fixed values of the coupling and charge parameters ($\alpha = 10^{11}$, $\hat{f} - 1 = 10^{-8}$), the maximum field and energy are computed for several values of the ratio r_{b2}/r_1, and the results are plotted in Figures 13 and 14.

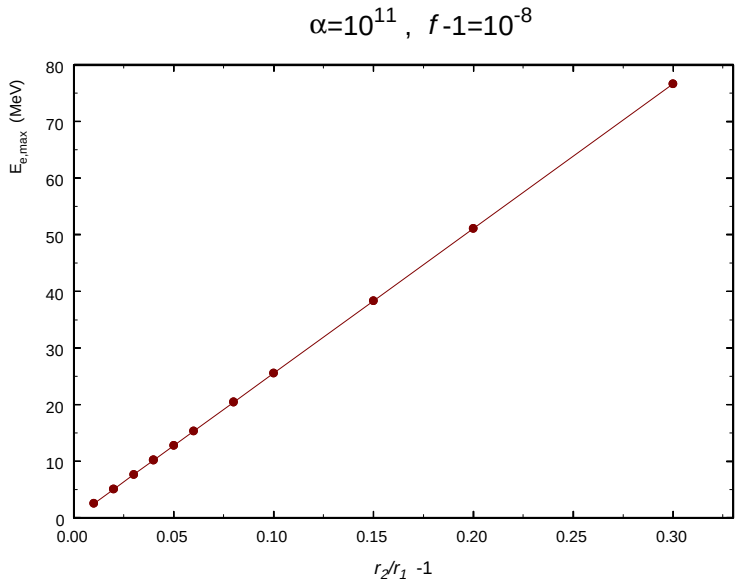

Figure 13: Scaling of electron energy versus shell thickness.

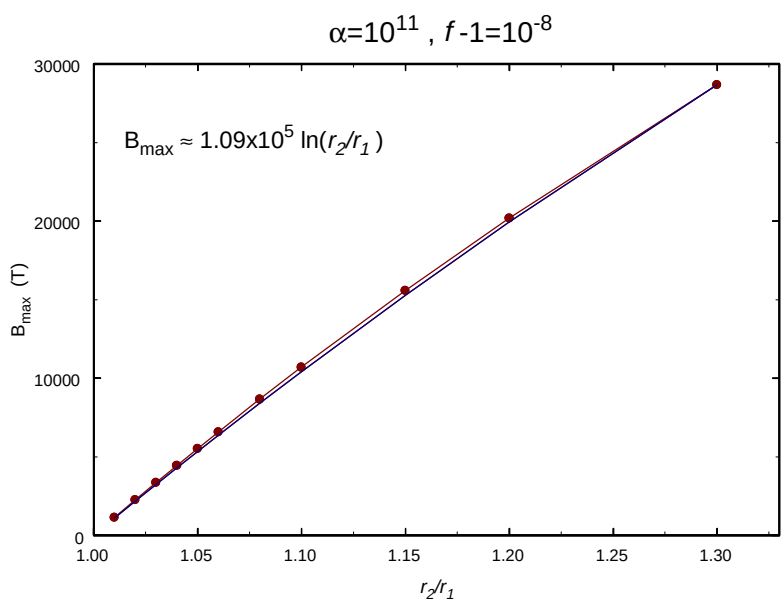

Figure 14: Scaling of magnetic field with size ratio. Both data and approximate fit shown.

It appears then that the electron energy scales exactly with the normalized shell thickness $r_{b2}/r_1 - 1$. The scaling behavior for the magnetic field is more complex, and the formula shown in Figure 14 is an approximation. Since the peak electron energy is obtained at the outer edge (where the field vanishes), a simple scaling relationship can be obtained for the velocity. From (22), we have at the boundary:

$$v_e \propto \left(\hat{f}-1\right)^{1/2}\left(\frac{r_{b2}}{r_1}\right)^{1/2}\left(1-\frac{r_1}{r_{b2}}\right)^{1/2} \tag{66}$$

converting to physical variables and expressing the energy ($E_e = \frac{1}{2} m_e v_e^2$), we finally obtain:

$$E_{e,\max} \propto \alpha\left(\hat{f}-1\right)\left(\frac{r_{b2}}{r_1}-1\right) \tag{67}$$

which is confirmed by both Figures 12 and 13. Combining all the data, the following approximate scaling relationships can be obtained:

$$E_{e,\max} \approx 2.56\times10^5\left(\frac{r_{b2}}{r_1}-1\right)\left(\frac{\alpha}{10^{11}}\right)\left(\frac{\hat{f}-1}{10^{-8}}\right) \quad \text{keV} \tag{68}$$

$$B_{\max} \approx 1.09\times10^5 \ \ln\left(\frac{r_{b2}}{r_1}\right)\left(\frac{\alpha}{10^{11}}\right)\left(\frac{\hat{f}-1}{10^{-8}}\right)^{1/2} \quad \text{Tesla} \tag{69}$$

Although the electron energies in the EST can be quite high, it is <u>assumed</u> that the temperature is very low (i.e., the electrons are monoenergetic). In that case, the coupling parameter can be large:

$$\Gamma = \frac{1}{kT}\frac{e^2}{4\pi\varepsilon_o R} > 170 \quad \text{, with} \quad R^{-1} = \left[\tfrac{4}{3}\pi\, n\right]^{1/3} \tag{70}$$

This implies that $T \approx 2^o K$ and presents another engineering challenge. For example, refs. [2,3] describe EST formation with an "injected" electron beam. It is not clear how EPS proposes to generate an electron beam and capture it in a shell with a relative energy spread of less than 10^{-8}. There is also some confusion regarding the EST production method; in [5] an electric arc is mentioned instead. The arc should have an even higher energy spread.

7. Energy Storage and Lifetime

The EST parameters listed in [2] are different from the cases studied above and in [1], and since there is some missing information, one cannot extract the exact relevant quantities. Nevertheless, the right orders of magnitude can be obtained. The relevant parameters are listed in Table 3.

Diameter, major, r_T:	0.63 m
Diameter, minor, r_o:	0.21 m
Electron energy:	10 keV
Total Mass:	1.86×10^{-6} kg
Magnetic Field:	16,000 Tesla
Energy Loss, Radiation:	1.16 J/sec
Energy Loss, Collisions:	8.9×10^{-10} J/sec
Total Energy:	1.9×10^{12} J

Table 3: EST parameters listed in [2].

It is not clear how these values have been obtained, and there are some inconsistencies. First, the list mentions diameters, while symbols for radius are used. Assuming a hydrogen plasma, the total mass gives a total number of ions (and electrons): $N_i \approx N_e \approx 1.12\times10^{21}$. Since there is no information concerning the shell thickness, it is necessary to assume a value. Choosing $r_{b2} = 1.05\, r_1$, the plasma volume is of the order of 6.7×10^{-3} m, and the electron density is therefore: $\bar{n}_e \approx 1.7\times10^{23}\ \mathrm{m}^{-3}$. The plasma frequency is then $\omega_{pe} \approx 2.3\times10^{13}\ s^{-1}$, and the corresponding coupling constant (assuming the inner radius is r_1=0.21 m) must be $\alpha \approx 2.6\times10^{8}$. The plasma frequency also corresponds to an equivalent field of $m_e\omega_{pe}/e \approx 132\ \mathrm{T}$. This is in marked contrast with the claimed value of 16,000 T given in [2]. Although some numerical solutions (not shown) have a peak value of the normalized cyclotron frequency $\hat{\Omega}_{ce} > 1$, they have all been found to be of the same order. This is where the scaling relations can be useful. Inverting (68,69), one finds:

$$\left(\frac{\hat{f}-1}{10^{-8}}\right)^{1/2} = 0.426\left[\frac{E_{\max}(keV)}{B_{\max}(T)}\right]\frac{\ln(r_2/r_1)}{r_2/r_1-1} \tag{71}$$

$$\left(\frac{\alpha}{10^{11}}\right) = 2.155\times10^{-5}\left[\frac{B^2_{\max}(T)}{E_{\max}(keV)}\right]\frac{(r_2/r_1-1)}{[\ln(r_2/r_1)]^2} \tag{72}$$

Considering two typical values for the relative shell thickness, 1.01 and 1.05, and using the claimed values of $E_{\max}$ and $B_{\max}$ in Table 3, one finds:

r_2/r_1	α	f -1
1.01	5.57×10^{15}	7.0×10^{-16}
1.05	1.16×10^{15}	6.7×10^{-16}

Table 4: Typical structural parameters satisfying energetic values in Table 3.

A search in parameter space in the case $r_2/r_1 = 1.05$ yielded the "best" numerical solution (i.e., one with $E_{e,\max}$ =10 keV and $B_{\max} = 16{,}000\ \mathrm{T}$) for $\alpha \approx 1.9\times10^{15}$ and $\hat{f}-1 \approx 5\times10^{-16}$, very close to the values predicted by the scaling laws. These values for the coupling constant are 8 orders of magnitude greater than the one derived from the mass of the system! Furthermore, these values correspond to an electron density $\bar{n}_e \geq 6\times10^{29}\ m^{-3}$. This is higher than solid-state densities (the number density for solid copper is 8×10^{28}, while it is 3×10^{28} for water)! Any error in the scaling relations (62,63) would reside in the scaling of the magnetic field with respect to the shell size. As seen in Table 4, the effect of size is limited. One must then conclude that the values of magnetic field, energy, and mass given in [2] are incompatible with each other, as well as with the numerical solutions[†].

The next step in the analysis is to examine the rate of collisions in the system. Since the electrons and ions are not separated in the model described in [1], the electrons will loose energy through Coulomb collisions with the ions. The only way these collisions could be prevented is if the ions were moving at the same velocity, in which case there would be no current generated, as well as no magnetic field. An expression for the rate of energy loss is found in [11], p.41:

[†] It is emphasized here that the problem is not so much with the absolute scale of the density, although astonishing in its own right, but with the severe inconsistency of the parameters.

$$\frac{dE_e}{dt} = -n_i \frac{Z_i^2 e^4 b_i \ln\Lambda}{4\pi\varepsilon_o^2 m_i} H(x, m_i/m_e) \tag{73}$$

where E_e is the energy of the electron, $b_i = (m_i / 2kT_i)^{1/2}$, and $\ln\Lambda$ is the Coulomb logarithm. For electron-ion collisions:

$$\ln\Lambda \approx 31.3 - \tfrac{1}{2}\ln(n_i) + \ln(T_i) \tag{74}$$

The function H is defined by:

$$H(x,\mu) = erf(x)/x - 2\pi^{-1/2}(1+\mu)\exp(-x^2) \tag{75}$$

with

$$x = b_i u_e = \left(\frac{m_i E_e}{m_e T_i}\right)^{1/2} \tag{76}$$

with E_e and T_i expressed in the same units. For the parameters listed in Table 3 and assuming a hydrogen plasma at $T_i \approx 2^o K$, we have $x \approx 3.4\times10^5$. For large values of x, $H \approx 1/x$. Using the *low* value of density derived from the mass ($n_i \approx 1.7\times10^{23}$) and $\ln\Lambda \approx 7.35$, the final result is:

$$\frac{dE_e}{dt} \approx 10^{-12} \text{ J/s} \approx 7000 \text{ keV/s} \tag{77}$$

This is the rate of energy loss for *each electron*. To find out the rate of energy loss for the entire torus, it is necessary to multiply by the total number of electrons, which is approximately $N_e \approx 1.1\times10^{21}$. Thus, the total rate of energy loss is approximately:

$$\dot{E}_{EST}^{col} \geq 10^9 \text{ J/s} \quad \text{for the entire EST} \tag{78}$$

Expression (77) implies that it takes approximately 1.4 msec for each electron to loose its energy. This corresponds to 300 orbits around the minor circle. Although the mean-free path is large compared to the dimensions of the system and the plasma can be considered "collisionless", the neglect of collisions is valid on the time-scales characteristic of the plasma dynamics. However, if one looks at long-term stability, the absolute rate of collisions must be considered. Another way to evaluate the rate of collisions is to look at the Rutherford scattering cross-section, i.e., the single binary collision for a deflection angle of 90° or more. For example, using expression (6.1.15) of ref. [12] or (9-10) of ref. [10], the cross-section for such an event is approximately $\sigma_{90} \approx 10^{-26}$ m^2. This leads to a frequency of events 10^5 s$^{-1.}$ Since only a fraction ($\approx 2\delta$) of the electron energy is transferred during each such collision, the time required for complete relaxation of the electron energy becomes 10^{-2} sec. However, at these plasma conditions, the impact parameter for 90° deflections p_{90} is very small. The ratio of large to small angle collisions is then [10]:

$$\left(\frac{p_{90}}{\lambda_D}\right)^2 \approx 10^{-7} << 1 \tag{79}$$

and the expression (73) for multiple collisions is more appropriate. Therefore, one expects the rate of energy loss to be given by Equation (78), but it could be much larger if the density were to be consistent with the scaling relationships obtained from the numerical solutions. Note that EPS claims a rate of 10^{-9} J/s for the entire EST, a difference *of 18 orders of magnitude*!

To emphasize the consequences of this, consider the following. Assuming the rate of energy loss is indeed given by the value in Table 1, the rate of energy loss per electron becomes:

$$\frac{dE_e}{dt} \approx 8\times10^{-31} \; J/s \tag{80}$$

for the entire system.

This rate would be obtained for a number density of the order of 10^{23} m^{-3}. Since the rate scales linearly with the number density of ions and if the number density was of the same order as the number density of copper[†], the rate of energy loss per electron would be:

$$\frac{dE_e}{dt} \approx 3.8\times10^{-25} \text{ J/s} \approx 2.3\times10^{-9} \text{ keV/s} \tag{81}$$

It would therefore take 4×10^9 sec for the 10 keV electron to loose its energy, which implies that such an electron beam would be able to go through 4×10^{13} km of solid copper without stopping!

One could argue that the loss-rate by collisions (given by Equation (73)) is a *local* quantity and should be evaluated through volume integral, rather than using global and maximum values for the density and electron energy. Although the density varies as r_1/r, the range of variation is small (since $r_{b2}/r_1 \leq 1.05$), thereby providing at most a 10% change. However, the variation of the electron energy is much more rapid and could make a difference. Therefore, the numerical integration procedure was modified to include a volume integration of the collisional losses. One should point out first that for $m_i/m_e \approx 2000$, the function *H(x)* has a maximum near $x \approx 3$ and can be approximated as $1/x$ beyond that. Using local values ($x \geq 3$) only in the integration, one finds that the volume integration gives a result within 25% of the result (78) obtained from global and peak values. Using $x \geq 10$ values only in the integration gives results larger by one order of magnitude. Because the Coulomb collision cross-section increases as the electron energy decreases, using the peak value of electron energy in (73) for a global estimate yields a value that underestimates the actual rates of energy losses by collisions with ions. It is therefore clear that the value claimed in [2] is unphysical in a dramatic way if the ions and electrons are co-located, as indicated by the theoretical model of the EST of [1].

It was suggested by EPS that the EST surface should be considered as a strongly coupled system with collective behavior, and that particle-particle collisions do not apply. However, this suggestion is at odds with the fundamental physics involved. It is true that the electrons in the collective state do not "collide" with each other, and if the ions also form a strongly coupled plasma, ion-ion collisions are also removed. However, the ions and electrons *together* do *not* form a strongly coupled plasma! The condition (70) for strong coupling is not satisfied for the electron-ion system, because the relative difference in energy (10 keV) between ions and electrons is far too large. Therefore, high-energy electron-ion collisions definitely occur. The situation can be better visualized with the following analogy. Consider a metallic solid with a conduction band or an ionic crystal. The system can be thought of as an ion component in a lattice (strongly coupled plasma) with a neutralizing background of electrons. Collisions between ions do not occur in this system; only *collective* excitations (in this case, phonons) are naturally present. Yet, if a 10 keV atomic beam is directed at the solid, one is guaranteed to have a lot of individual particle collisions with a significant amount of ions ejected from the solid. The case of the EST is similar. Ions and electrons would respectively form lattices at near solid density, but impacting each other at high velocities. Because the relative kinetic energy between the two components is large, particle collisions frequently occur and are correctly described by Equations (73) through (81).

The radiative losses should also be considered. The rate of cyclotron emission can be obtained[†] from ref. [11] again (p. 68):

$$P_c = 6.21\times10^{-17}\ n_e\, T_{e(keV)}\, B^2 \quad \text{W/m}^3 \tag{82}$$

[†] Although solid copper is not a plasma per se, the Rutherford cross-section would still apply at these high energies.

[†] Strictly speaking, since the electrons are mono-energetic, one could use the radiated power emitted by a single electron, using classical formulas such as (14.31) of [13]. However, this does not affect the discussion.

Here, $T_e \approx E_e$, and this gives a rate of total energy loss by cyclotron emission for the EST:

$$\dot{E}_{EST}^{cyclo} \approx 6.95\times10^{5}\ B^{2} \quad \text{J/s} \tag{83}$$

If the field is 16,000 T as claimed, the rate of energy loss by cyclotron emission is:

$$\dot{E}_{EST}^{cyclo} \approx 1.8\times10^{14} \quad \text{J/s} \tag{84}$$

again a difference of 14 orders of magnitude with the rate claimed in [2] (see Table 3). However, this would be a gross overestimate of the emitted power, since the highest electron velocities are in a region near the outer edge of the plasma shell where the magnetic field is small. To correctly evaluate the cyclotron radiative power, the numerical integration scheme was modified to include an integration of the cyclotron power. A solution of the dynamical equations was chosen such that the maximum field was 16,000 Tesla and the maximum electron energy 10 keV, for the same size as the EST configuration given in Table 3. Of course, the corresponding plasma densities and total number of electrons were much higher than those derived from the EST mass, following the approximate scaling relationships discussed above. The total emitted power for this solution was:

$$\dot{E}_{EST}^{cyclo} \approx 4\times10^{7}\ \text{J/s} \tag{85}$$

while Equation (82), using the maximum values globally, would give 10^{22} J/s. Therefore, there is a large reduction in emitted power when the correlation between electron energy and magnetic field is taken into account. Nevertheless, the solution gives a cyclotron power much larger than the one quoted in [2]. However, it would become of the same order if the results were scaled to match the density obtained from the EST mass. Therefore, the cyclotron power emitted may be correct, but the quoted magnetic field value is in serious disagreement with the numerical solutions and the scaling laws.

The total energy can be evaluated as the magnetic field times the total volume of the torus, i.e.:

$$E_{EST} = \left(2\pi^{2} r_b^{2} R_T\right)\left(\frac{B^{2}}{2\mu_o}\right) \tag{86}$$

Assuming $B \approx 16{,}000\ \text{T}$, the total energy is 6×10^{13} J. Even if the sizes given in Table 3 were the actual diameters instead of radii, the energy would be 7×10^{12} J. This is still larger than the value mentioned in [2] and listed in Table 3, yet another inconsistency in the claimed results. It can be easily verified that the kinetic energy of the electrons is negligible compared to the magnetic energy. If the rates of energy losses given in [2] were used, the EST would have a lifetime of 50,000 years! Using the loss rate from Equation (78), the EST would last about 7000 sec, still an extraordinary achievement in terms of plasma stability. However, the true collisional lifetime is given by the electron energy lifetime itself, which according to Equation (77), is only on the order of a millisecond.

Therefore, it is clear that collisions between electrons and ions would prevent the EST to achieve the very long claimed lifetimes. Of course, this is a problem if the electrons and ions are both located in the same regions, which is a key assumption in the model described in [1]. Since this model was repeatedly mentioned as an independent description of the physics of the EST, it is then reasonable to assume that it is the current state-of-the art in the theoretical description of the EST. In fact, as mentioned in Section 4 regarding the ion dynamics, there is no clear description of the ion properties anywhere else in the literature [2-3]. The new version of a document [5] explicitly mentions the separation of ions and electrons. This is a new addition, made after a preliminary version of the present report was made available to EPS.

Separation of ions and electrons is possible in some cases. As pointed out by Seward [2,3], strongly coupled one-component plasmas can organize themselves in shell-like structures, as

demonstrated by Gilbert et al [14] for an ion plasma in a Penning trap (i.e., confined by an strong external magnetic field). Strongly coupled plasmas are now commonly created in the laboratory, although always in the presence of confining field configurations such as Penning and Malmberg traps. Strong coupling is indeed a key assumption[†] of the EST model, thereby implying that the ions and electrons form two distinct components, each one at low temperature. In fact, the coupling condition $\Gamma > 170$ for EST is typical of a solid-like plasma phase, corresponding to Coulomb crystal structures [15] rather than fluid-like shells, and it is probably more stringent than necessary. Due to the large mass difference between ions and electrons, one could then expect ion and electron shells to be separated. However, no one has yet realized such a two-component system. Furthermore, the realization of strongly coupled plasma configurations is rather delicate and currently requires cooling to very low temperatures in the presence of external confining fields. To expect that such structures can be formed from high-energy beams or electric arcs is yet another formidable claim that demands extensive proof. Finally, the ion shell would also be fundamentally unstable, since the system is globally charged with the relative excess of ions. Therefore, the ion shell would not remain separate from the electrons, and again, the collisions between electrons and ions would be unavoidable.

The ion confinement problem remains a key issue with important consequences. For example, suppose that the ions reside in a shell interior to the electron shell. If mechanical pressure is required to confine the ions, as now suggested by EPS [4], there must be a significant number density of neutrals at the edge of the ion shell and therefore <u>within</u> the electron shell. Then, the collisions between electrons and neutrals become inevitable, and at this range of electron energies (10 keV), the previous classical analysis remains relevant. Therefore, excessive collisional energy dissipation (with both ions and neutrals), remains an important problem that prevents any possibility of long lifetimes for any EST configurations.

After mentioning the need for a confining force provided by an external pressure, EPS again modified the theoretical model and stated [4] that there is a fixed ion background. The latter would be provided by an ionization process of the neutral particles diffusing inside the EST. In that case, electron-neutral collisions must be considered. The range data [16] of 10 keV electrons in air specifies a figure of 19.7 MeV.cm^2/g from which one can derive the electron-neutral *elastic* collision cross-section to be of the order of 10^{-20} m^2. If the neutral density were of the same order as the ion density in the EST, the electron lifetime would be 10^{-8} sec. If instead, only a partial pressure of 1 μTorr is present, the lifetime would be approximately 50 msec. This is still significantly less than the 10^6 hours claimed in [2]. At this point, it becomes important to evaluate the actual neutral partial pressure that would be required to maintain the EST in this scenario. This was already done in Section 5, thereby leading to a relationship between the external pressure and the magnetic field pressure, Equation (65). Another approach is now used, and again, the case of high-energy EST (Table 3) is examined.

The electrostatic confinement of the electrons (from the excess ionic charge) is responsible for the presumed generation of the large magnetic fields inside the EST (16,000 T in this case). From energetic considerations, if the field energy is much larger than the kinetic energy of the plasma, one should expect a balance between the magnetic field energy density ($B^2/2\mu_o$) and the energy density (or pressure) of the electrostatic field ($\varepsilon_o E^2/2$). As the former decreases near the edge, the latter increases. This indicates that the electric field at the edge of the shell is of the order of 5×10^{12} V/m. Another evaluation comes from the total charge of the EST, quoted in [2] to be 186 Coulombs. Assuming a cylindrical shape, the field would be:

[†] It is <u>not</u> a derived condition, as implied in some of the EST literature.

$$E \approx \frac{(Q/2\pi R_T)}{2\pi r_b} \approx 1.6\times 10^{13}\ V/m \tag{87}$$

These two approximations are in fairly close agreement. One can then consider the steady-state dynamics of the ions near the edge of the shell. The magnetic field vanishes in that region, and the electric field provides a large acceleration, while the collisions with the neutrals provide a frictional force, i.e.:

$$v\frac{dv}{dx} = \frac{eE}{m_i} - \nu_{in} v \tag{88}$$

where x is the distance along the ion path. Since the collision frequency between ions and neutrals also depends on the ion velocity ($\nu_{in} = N_n \sigma_{in} v$), an approximate solution can be found of the form:

$$\frac{v^2}{2} = \frac{eE}{m_i}\Lambda\left(1 - e^{-x/\Lambda}\right) \tag{89}$$

where $\Lambda = (2N_n\sigma_{in})^{-1}$ is the mean free-path. Note that as the magnetic field vanishes towards the edge of the shell, the Larmor radius becomes large, and the collision mean free-path becomes the relevant length scale[†]. The cross-section is typically of the order of 10^{-20} m^2, and if the gas pressure is 1μTorr at 300 K, the mean free path is 1,500 meters. The ions would therefore stream away from the EST at extremely high velocities without stopping, thereby invalidating the concept of partial vacuum confinement.

If the gas density is that of the presumed ion background inside the EST, the mean free path becomes 300 μm, which is a small fraction of the shell thickness. It would appear then that this is the range of neutral density required. A more accurate determination is shown below. It is interesting to also point out that the velocity gain during this distance is (according to (89)), about 7×10^8 m/s! This value is approximately the same as the one obtained from the $E\times B$ drift velocity, using peak values of both fields.

It was previously mentioned how energetic considerations dictate that the neutral gas pressure, in order to confine the ions, should be of the same order as the electrostatic energy density in order to confine the ions; i.e., of the order of 2.5×10^9 atmospheres for the EST described in [2] and Table 3. A similar result can now be obtained from kinetic considerations. Equilibrium is achieved when the momentum fluxes at the EST interface can be achieved. The ions inside the EST are accelerated to high velocity from the electric field, and the velocity at the interface can be obtained from (89) using an average over a mean free path. The representative distance is therefore $\Lambda/e \approx \Lambda/3$, and the average ion velocity at the EST boundary is:

$$v \approx \left(\frac{2eE}{3m_i}\Lambda\right)^{1/2} \tag{90}$$

The ion momentum flux across the interface is $N_i(m_i v)v$ and must be balanced by the corresponding flux from the neutral background (see Figure 15), i.e.:

$$N_i(m_i v)v = N_n(\overline{m_n v_x^2}) = N_n k T_n \tag{91}$$

where the statistical average ($\overline{v^2}$) over the neutral particle distribution has been used. Using (87), the required neutral pressure then becomes 9×10^{13} Pa, or 900 million atmospheres; again of the same order as the magnetic field pressure.

[†] Even using the Larmor radius for peak magnetic field does not actually alter the conclusions.

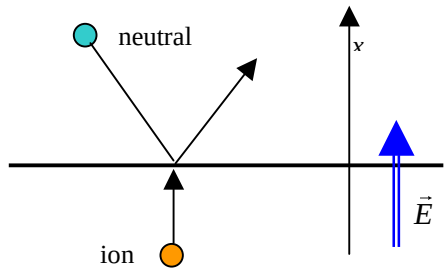

Figure 15: Schematic of kinetics at the EST interface.

More information can be gained from this elementary analysis. If the scenario of confinement by external pressure is abandoned and one relies instead on the ionization approach to maintain a fixed ion background, the actual rate of ionization can now be estimated. Again, using (90), the average ion velocity at the interface can be evaluated at $\approx 5\times10^{8}$ m/s. Using the actual dimensions of the EST (Table 3) and the inferred density, one can then evaluate the rate of particle loss. This is found to take the staggering value of: 10^{32} particles/sec. Since it takes at least 13.5 eV to ionize the gas, this corresponds to an energy loss rate of approximately:

$$\dot{E}_{EST}^{ioniz} \approx 2.3\times10^{14} \quad \text{J/s} \tag{92}$$

again a difference of 14 orders of magnitude from the claim made in [2]. Since this energy loss directly affects the kinetic energy of the electron component ($\approx10^{21}$ electrons $\times$ 10 keV), it is found to correspond to an EST lifetime of less than 10^{-8} sec, compared to the 10^{6} hours lifetime claimed in [2].

In a more recent document [8], Chen claims that the EST confinement is not incompatible with the Virial theorem. However, this statement deserves to be investigated in more detail, since the conditions necessary for this to occur still make the concept of long-term stability of a free EST nonfeasible. One must first start with the complete description of the Virial theorem:

$$\frac{1}{2}\frac{d^2 I}{dt^2} = 2(E_{kin}+E_{thr}) + E_{elec}+E_{mag} - \int_V d^3x\, x_\alpha \frac{\partial G^\alpha}{\partial t} - \int dS_\beta\, x_\alpha (p^{\alpha\beta}+T^{\alpha\beta}) \tag{93}$$

where I is the moment of inertia of the plasma, E_{kin} is its kinetic energy, E_{thr} is the thermal (or random kinetic) energy, and E_{elec}, E_{mag} are the energies of the electrostatic and magnetic fields respectively. If the plasma is a collection of particles of various types σ, the following definitions apply:

$$I = \sum_\sigma \int_V m_\sigma n_\sigma r^2 d^3x \tag{94}$$

$$E_{kin} = \sum_\sigma \int_V m_\sigma n_\sigma \left(\frac{d\vec{x}}{dt}\right)^2 d^3x \tag{95}$$

$$E_{thr} = \sum_\sigma \int_V m_\sigma n_\sigma \left\langle (\vec{v}-\vec{u})^2 \right\rangle d^3x \tag{96}$$

where $\vec{u} = d\vec{x}/dt$ is the mean plasma velocity. The field energies are of course given by:

$$E_{elec} = \int_V d^3x \frac{\varepsilon_o \vec{E}^2}{2} \tag{97}$$

$$E_{mag} = \int_V d^3x \frac{\vec{B}^2}{2\mu_o} \tag{98}$$

The radiation momentum density vector $\vec{G}$ and Maxwell stress tensor are given by:

$$\vec{G} = \varepsilon_o \vec{E} \times \vec{B} \tag{99}$$

$$T^{\alpha\beta} = \left(\frac{\varepsilon_o \vec{E}^2}{2} + \frac{\vec{B}^2}{2\mu_o} \right) \delta^{\alpha\beta} - \left(\varepsilon_o E^\alpha E^\beta + \frac{B^\alpha B^\beta}{\mu_o} \right) \tag{100}$$

For a sufficiently collisional plasma, the mechanical pressure tensor $p^{\alpha\beta}$ only has a diagonal component $p = nkT$. For a plasma in steady state, the moment of inertia is zero, i.e., the plasma neither expands ($d^2I/dt^2 > 0$) nor contracts ($d^2I/dt^2 < 0$). Assuming also that the plasma is at rest ($E_{kin} = 0$) and using the relationship between pressure and thermal energy, the condition for stability becomes:

$$3pV + E_{elec} + E_{mag} = \int_V d^3x\, x_\alpha \frac{\partial G^\alpha}{\partial t} + \int dS_\beta\, x_\alpha T^{\alpha\beta} + 4\pi R^3 p_{ext} \tag{101}$$

where the boundary term for the mechanical pressure was computed assuming the plasma volume as a sphere of radius R. The first term on the right-hand-side of (101) describes the effect of the radiation of electromagnetic energy: it physically corresponds to the "recoil" from the emission of photons. The second term describes the electromagnetic stress provided at the boundary by an external (confining) electromagnetic field. The third term is the effect of a mechanical pressure. If the plasma does not radiate and if there are no external fields or pressure, the RHS of (101) is identically zero. Since all terms on the LHS are positive definite, the stability condition cannot be satisfied, and the plasma is unstable (it expands). This is the origin of the impossibility of self-confinement of a plasma. Chen claims that these RHS terms are not necessarily vanishing, and can therefore provide a method of confinement. However, as we shall see, these terms would need to be very large.

Let us first consider confinement by radiation. According to [1], the Poynting vector due to coherent perturbations of the field at the surface of the EST is:

$$S = \frac{1}{2} \delta E_\phi \delta B_\theta e^{2\,\mathrm{Im}(\omega)t} \tag{102}$$

It is of second-order with respect to the perturbations and therefore very small. Furthermore, for stable configurations, Im(ω)<0; and the radiation decays exponentially in time. The same can be said for the momentum density vector $\vec{G}$. Chen uses the same coherent perturbations for the contribution of the Maxwell stress tensor at the boundary, and these are also of the same type. Therefore it is difficult to see how second-order perturbations, decaying exponentially in time, would contribute to long-term stability of the EST! Generally speaking, there is a fundamental problem with invoking radiative processes to provide a confinement mechanism. Physically speaking, conservation of momentum during the emission of radiation provides the mechanism for preventing the plasma particles to escape the system. Thus, if there is a net radiative momentum outward flux, the recoil of the plasma keeps it momentarily stable. However, the momentum of a photon is a rather small quantity ($h\nu / c$). In order to keep the EST confined, a tremendous amount of power would need to be radiated (c times the momentum flux!). The radiative losses would therefore lead to an extremely rapid collapse of the plasma.

The other term mentioned by Chen is the contribution of the external mechanical pressure. However, it is easy to see that this pressure must be large. Neglecting the radiative terms, one can see that in order to have confinement:

$$p_{ext} = p + \frac{1}{3}\left(\frac{\varepsilon_o E^2}{2} + \frac{B^2}{2\mu_o}\right) \tag{103}$$

Therefore, the external pressure must be of the same order as the energy density stored inside the EST, as discussed previously. It is difficult to imagine how Chen proposes to confine a high-energy EST with an internal magnetic pressure of 1 billion atmospheres in partial vacuum.

It is clear that none of the documented or potential explanations provided by EPS for the claims of stable energy storage is physically possible. So far, a valid theoretical model that can account for the experimental observations remains elusive. The extraordinary claims regarding the properties of the EST as well as the theoretical procedures utilized by EPAS are at odds with the known relevant physics. One could be tempted to assume that, although the theoretical models provided by EPS are in error, there could be experimental evidence of some structure. However, based upon the additional documentation provided by EPS, there are also some problems with this type of evidence, as described in the next section.

8. Experimental Observations

Among the additional documentation furnished by EPS was a report to the defense Special Weapons Agency (DSWA) [6], which included a slightly more elaborate description of the experimental procedure used to create ESTs. In the 1999 version of an EPS document [3], EST initiation is described in terms of electron beam injection, while in the 2000 version [5] an electric arc is used. There is also a mention in [6] of generating the ESTs by using an exploding wire. The electric arc approach is described in [6]. In a tabletop experiment, a high-current arc discharge (400 amps) between two carbon electrodes is initiated in a low-pressure (0.0011 atm) Nitrogen atmosphere. The experiment lasts 10 seconds and is characterized by electrode material vaporization and the melting of parts of the structure. Pictures of the experimental set-up show significant thermal damage. The "proof" of the presence of ESTs consists of a picture of a small, luminous ring-like object seen at some distance from the arc. It is not clear whether this is an EST or another more benign structure, since there is no measurement of some of the key characteristics of the EST. For example, plasmoids (neutral plasma structures with toroidal configurations), have often been generated [17] and have demonstrated (relatively) good stability properties, although certainly not on the level claimed in [2-6]. There is also repeated mention of the charge neutrality of the EST, since it is not affected by the electric field. This would then also imply that there is no significant energy storage or magnetic field trapped within the torus, since the two are closely related.

An energy loss rate of 1.89×10^{-7} joules/m^2 of surface area (assuming that the authors meant *watts*/m^2) is quoted [6] and claimed to be an important result that demonstrates the stability of the EST. It is worth looking at this in more detail. The luminous power of the EST is obtained in [6] by visually comparing it with that of a Light Emitting Diode (LED) and is (taking into account a geometric factor) of the order of 0.0026 watts[†]. The EST has a major radius of 3.5 mm and a minor radius of 1 mm, thereby giving it a shell surface area 1.38×10^{-4} m^2. Dividing the total emitted power by the surface area, one should then obtain an intensity of 19 watts/m^2. The result of 1.89×10^{-7} joules/m^2 claimed in [6] is obtained by *multiplying* (instead of *dividing*) by the

[†] Again, the units used in [6] were Joules for a rate, instead of watts, or J/s.

surface area! This "important result" of low energy loss rate is therefore incorrect by 8 orders of magnitude. This error has since been corrected by EPS.

In the same reference ([6], p. 11), a "demonstration" EST is described with characteristics similar to the one "observed" in the arc experiment, at least as far as the electron energy (110 eV, of the order of the energy acquired in the cathode layer) and the ambient atmosphere are concerned. However, the major radius is now 10 cm, while the radiative power is now 0.00046 J/s. It is not clear how a total radiative power 10 times *smaller* than the experimental one could be obtained when the surface area is 3000 times *larger* than the (assumed) experimental EST.

It is then further stated that the number of ions is approximately 1% greater than the number of electrons. This is in disagreement with the values quoted in the same document for the analysis of the experiment. In this analysis, Chen quotes a value for the relative charge excess: $\hat{f}-1 \approx 7\times10^{-5}$, which is significantly different from the 1% mentioned elsewhere. It is also worth looking at this experimental analysis in more detail. A key assumption in Chen's analysis is that the background ion density is equal to the ambient density, which is approximately $\bar{n} \approx 2.5\times10^{22}$ m^{-3}. Using this value for the electron density and the given EST dimensions, this corresponds to $\alpha \approx 890$, which is close to the value ($\alpha \approx 1100$) quoted by Chen. Another assumption is that the maximum electron energy is 200 eV. Using this value and the computed value of α with the scaling relation (37), one finds that $\hat{f}-1 \approx 8.7\times10^{-5}$, again close to the value quoted by Chen. However, there are two other important pieces of information concerning the experiment that are important to mention:

- The observed ESTs appear to be charge-neutral, since they do not appear to be affected by the electric field near the electrodes.

- The EST's are affected by gravity, and are seen to follow parabolic trajectories.

The latter can provide some information about the typical acceleration to which the EST is subjected. Using a characteristic dimension of $L = 10$ cm (the average interelectrode separation) and an EST lifetime of 0.6 sec, the acceleration must be at most of the order of:

$$a_{buoy} \leq \frac{2L}{t^2} \approx 0.5 \text{ m/s}^2 \tag{104}$$

Note that this corresponds to an average mass density in the EST only 5% larger than the ambient density, which is consistent with Chen's assumption. However, the acceleration in an electric field is simply given by:

$$a_{elec} \approx (\hat{f}-1)\frac{e}{m_{N_2}}E \tag{105}$$

where m_{N_2} is the molecular mass of nitrogen. With the applied voltage of 200 Volts used by Chen and an interelectrode spacing of 10 cm, this leads to:

$$a_{elec} \approx 5\times10^5 \text{ m/s}^2 \tag{106}$$

In order to match the observation that the EST is "charge-neutral" (i.e., is not affected by the electric field), the acceleration from the field should be much less than the one due to gravity. However, according to the parameters deduced by Chen, it is *6 orders of magnitude* larger.

Therefore, it is clear that this document provides no reasonable evidence supporting the existence of the high-energy EST (i.e., one with a significant electric charge). However, a completely

charge neutral structure (and therefore probably not an EST) is not ruled out. It is also interesting to point out that a rate of energy losses by collisions was given for the very high energy EST described in [2], which is extremely low to support lifetimes of the order of several years. It is not clear how this value was obtained. As demonstrated earlier, if the same theoretical model [1] used to describe the properties of this EST is utilized, the collisional losses mentioned in [2] are 18 orders of magnitude below the expected levels. If the ions and electrons are separated as claimed in the more recent documentation [5], there are no collisional losses; however, the ion confinement remains a daunting problem. If neutrals must exert a confining pressure on the ion shell inside the torus, then electron-neutral collisions are unavoidable and the energy losses are again large. If the losses are estimated from the experimental data (assuming that the observed structures are ESTs) and using the rate of energy loss per unit of EST surface area the results are underestimated by at least 8 orders of magnitude as shown above. Despite claims to the contrary, there is no justification for assuming a low rate of energy loss of the EST.

In a recent meeting between MSE, EPS and MIT [7], additional experimental evidence was presented. Primarily, this consisted of photographs of toroids produced in arc experiments and in exploding wire experiments. The latter method appeared to produce a much larger number of toroids (the assumed EST) than the arc method. An interesting parametric study was also performed by EPS with respect to the appearance of the toroids. In that study, a photographic image was simulated, assuming a toroidal plasma shape and various rates of rotation along major and minor axes. This study was then able to provide the range of rotation speeds required for the photographic image to always appear as it does in the experiments. This study was of great interest, because it provides the first example of valuable data against which various physical models of the plasma toroids can be compared. The study is definitely a step in the right direction. One key difficulty in the experimental investigations of the EST is the lack of diagnostics. This is of course related to the lack of reproducibility. Since the production of ESTs is an inherent random phenomenon, it is difficult to predict the time and location at which the EST is formed, and where advanced diagnostics could be applied. Therefore, it appears critical to proceed in two directions: 1) systematically investigate the conditions for maximal rate of EST production; and 2) perform systematic statistical analyses of the produced EST. The difficulties associated with EST characterization are duly appreciated. Nevertheless, it is strongly urged that further progress in this direction be undertaken, in order to provide useful experimental data to test **all** possible models of the observed phenomena.

9. Conclusions

Based upon the analysis of all the provided information, a number of conclusions can be made regarding the EST concept as proposed and observed by EPS. It is important to distinguish between the theoretical models and the experimental observations. It is <u>undeniable</u> that EPS does observe luminous toroidal structures in its experiments. However, the nature of these structures is far from clear. For example, one could simply assume that they are luminous fluid vortices ("smoke" rings) containing small particles at high temperature (the result of electrode or wire vaporization). Photographic snapshots could not provide enough information to eliminate this tentative explanation, but the study on rotation rates indicates that this is extremely unlikely (thus the usefulness of such studies, as mentioned earlier). However, a rigid structure cannot be ruled out. Other various complex, exotic and likely models can be proposed, as well. The cold-fluid, multishell model with a high magnetic field stored within the toroidal shell as proposed by EPS is rather extreme and (as described in this report) highly unlikely. However, there may be some hope of finding the correct physical model. Once this is done, potential applications can be accurately assessed.

MSE's conclusions regarding the analytical and experimental data published by EPS and MIT regarding the EST concept are as follows:

(1) The cold-fluid equations for the electron gas and their numerical solutions (described in [1]) have been verified. These equations are applied to a toroidal plasma shell in the approximation of a very large torus diameter ($R_T >> r_b$). The electron fluid rotates to create a magnetic field inside the torus, while being confined by the electrostatic field created by a excess of positive charges in the plasma. MSE's numerical solutions agree with Chen's on this point.

(2) However, the model in [1] **does not** describe the complete dynamics of the system. Within the context of that model, it is found that the ionic component is unstable in the presence of the required electrostatic field. Therefore, one cannot at the same time realize a configuration that confines both electrons and ions without invoking an external confinement mechanism. An external confining field would need to be of the same order as the field being stored inside the torus, thereby limiting practical applications of the concept.

(3) The discrete model proposed by EPS contains various fundamental errors. In the limit of a large number of electrons, the correct equations were provided by MSE and are consistent with the cold fluid model. Again, the ions cannot be naturally confined.

(4) An external mechanical pressure is required to confine the ions. This was mentioned by Chen after MSE provided a preliminary copy of the present analysis to EPS, but a small ("partial" vacuum) pressure was deemed necessary [4]. However, it can be seen from simple arguments and from the classical Virial theorem, that the confining pressure would need to be at least of the same order of magnitude as the energy density contained in the EST. Therefore, there is no possibility of confinement of high-energy ESTs in a partial vacuum.

(5) The other contributions to the Virial suggested by Chen [8], namely radiative emission and perturbations of the electromagnetic stress tensor at the boundary due to coherent fluctuations are not relevant. Physically speaking, it is pointless to use the radiative emission to prevent plasma expansion, since this would imply a very high rate of energy loss, thereby leading to a rapid collapse of the structure.

(6) The need for an external pressure (mechanical or electromagnetic) of the same order as the contained energy density is critical to the assessment of feasibility and usefulness of the EST concept. Any potential for large energy storage capability with no external field is negated, since the requirements for an external magnetic field are replaced by an equally impractical requirement for large neutral pressure.

(7) Using the current theoretical model of the EST, it has been shown that the mixture of ions and electrons would be the subject of excessive losses through Coulomb collisions and possibly cyclotron radiation. This energy loss rate is sufficient to prevent "long-term" stability of the plasma, even in the presence of an externally applied confining field. A modification of this model using separation of ions and electrons into separate "shells" would prevent these collisional losses but is not possible without a plausible mechanism for ion confinement. Since an external pressure would be required to confine the ions, electron-neutral collisions then become unavoidable and lead to similarly large and debilitating rates of energy losses.

(8) The mention by EPS [4] of suppression of electron-ion collisions due to the strong coupling is not valid. Since the relative velocity between electrons and ions is large, the electrons and ions together do not form a strongly coupled plasma.

(9) After further discussion [4], EPS stated that the fixed ion background was real and was the result of a continuous ionization process of the background neutrals. This process was also examined and found to be fundamentally flawed, leading to even greater rates of energy losses that are incompatible with any claim of long term stability.

(10) The numbers presented in the literature [2-6] are often inconsistent and at times unphysical. Furthermore, the analysis of the experiment presented in [6] is inconsistent with the observations. There is also no measurement of the essential physical properties of the EST, so other interpretations of the experiment cannot be eliminated.

Based upon these results, one must conclude that the EST concept (as currently proposed by EPS and MIT) is fundamentally flawed. None of the claims of extraordinary energy storage capability and absolute stability can be scientifically substantiated. Although the present analysis used the example of a high-energy EST for demonstration purposes, the conclusions affect EST configurations *on all scales*. Various tentative models for ion confinement and EST stability have been suggested by EPS, but none of these satisfies basic physical constraints. These claims were made before the problem of ion confinement had been seriously addressed. It is absolutely <u>essential</u> that this problem be resolved before long-term stability and energy storage properties can be accurately evaluated.

Although the documentation concerning the experimental evidence is limited, it also appears that a thorough analysis of the experimental data has yet to be performed. The experiment described in the provided reference [6] utilized inadequate diagnostic procedures. However, it should be pointed out that this is not necessarily the responsibility of the investigators, but rather the result of the chaotic nature of the phenomena and possibly the lack of adequate funding. This analysis is the most complete to date and used the very latest data and models suggested by EPS. It also exposed a number of fundamental problems, which had not been previously identified.

The principal objections to the EST concept as currently proposed by EPS concern the theoretical model, as well as claims of very large energy storage and stability properties as made by its investigators. Unfortunately, these claims divert attention from other possible physical explanations for the experimental observations. As emphasized earlier, the observed production by EPS of plasma structures in exploding wire and arc experiments is undeniable. Although this is not the first time that such plasma structures have been produced [18], the EPS observations are relatively new and can potentially benefit from better diagnostic procedures. The study of “Ball Lightning” [19] phenomena contains many similar observations, along with a large variety of theoretical models. Some of these models could also be invoked as an explanation for the experimental observations made by EPS. At any rate, the theoretical work done to date by the EPS/MIT team lacks completeness and accuracy. For example, the ion confinement problem was never mentioned before discussion with MSE, yet it is critical to long-term stability. Various mechanisms were proposed to address the stability problem, but none was found to be physically feasible. The current direction in theoretical development by MIT now seems to include a two-fluid model, yet it is not clear what could be expected from this new development. Instead, it seems clear from a look at the Virial Equation [e.g., Equation (101)] that the real problem concerns the lack of a negative energy term. For example, this is supplied in astrophysics by gravity such as in the cases of self-gravitating plasma rings [20]. In a degenerate plasma, the exchange energy plays a similar role, and this allows an ionic crystal to be stable. This would be an alternative possible approach to the classical fluid model. Of course, such a system could not allow the storage of energy in a magnetic field, since both the electrons and ions together would need to be strongly coupled (i.e., no relative velocity). This model could have some applications, although it would not be an EST (i.e., no magnetic field).

It should now be clear that there is no physically feasible solution for the EST concept which by definition includes high loop current, non-neutral plasma, and trapped magnetic field. As proposed, the energy storage applications are not possible. However, the possibility of charge neutral, metastable structures (lifetimes of the order of several milliseconds) is intriguing and can have a number of applications. Chen proposed to use such structures for propulsion, since their long lifetime (1 ms) might allow them to be accelerated to high speed. With the structure being charge-neutral, the only way to apply an accelerating force (as proposed by Chen) would require a gradient of magnetic pressure. However, to generate a strong gradient across the EST dimension (< 1cm) with an applied magnetic field would be a serious challenge.

MSE believes that the pursuit of stable (or rather, "metastable") and energetic plasma structures is a worthy and very important endeavor. Research in this direction should be pursued, but with much caution and under strict peer-review. A more determined and focused research program on theoretical model development should be a high-priority item. Despite the many problems with this EST concept, it is recommended that independent theoretical (using different models) and experimental investigations of the feasibility of using various plasma structures for propulsion or energy production should be initiated by NASA.

10. References

[1] C. Chen, "Equilibrium and Stability Properties of Cold-Fluid Electron Spiral Toroids", Electron Power Systems, Inc., 1999.

[2] C. Seward, "Low Cost Transportation using a Stable Plasma for Energy Storage", NASA report, NIAC-CP-98-01, May 1999.

[3] D. C. Seward, "Energy Storage Using the Electron Spiral Toroid", EPS Inc. pub., Sept 1999.

[4] C. Chen and C. Seward, private communication.

[5] D. C. Seward, "Energy Storage using the Electron Spiral Toroid", EPS Inc. pub., Jan. 2000.

[6] C. Seward, "The Electron Spiral Toroid (EST) for Energy Storage", Final Report to DSWA, October 1998. Contract # DSWA01-97-M-0537.

[7] C. Chen, C. Seward , D.C Seward and W.J. Guss, private communications, MSE/EPS/MIT Meeting, MIT, May 25, 2000.

[8] D. C. Seward, "Energy Storage using the Electron Spiral Toroid", EPS Inc. pub., May. 2000.

[9] C. Chen, "Equilibrium and Stability Analysis of Intense Electron Spiral Toroids", presented at the MSE/EPS/MIR meeting [7].

[10] G. Schmidt, *Physics of High-Temperature Plasmas*, Academic Press, NY, 1966.

[11] T. J. Dolan, *Fusion Research*, *Volume I – Principles*, Pergamon Press.

[12] N. Krall & A. Trivelpiece, *Principles of Plasma Physics*, San Francisco Press, CA, 1986.

[13] J.D. Jackson, Classical Electrodynamics, J. Wiley, New York (1975).

[14] S. Gilbert, J. Bollinger and D. Wineland, "Shell-Structure Phase of Magnetically Confined Strongly Coupled Plasmas", *Phys. Rev. Letters*, vol. **60**, 2022 (1988).

[15] See for example: S. Ichimaru, *Rev. Mod. Phys.*, vol. **54**, 1017 (1982).

[16] M. Berger and S. Seltzer, "Tables of Energy Losses and Ranges of Electrons and Positrons", NASA SP-3012 (1964).

[17] See for example: W. Bostick, "Plasmoids", *Sci. American*, vol. **197** (Oct. 1957).

[18] See for example: P. A. Silberg, *J. Appl. Phys*., vol. **49** (1978), 1110.

[19] See for example: "Science of Ball Lightning", ed. Y.H. Ohtsuki, World Scientific pub., Singapore, 1989.

[20] V.D. Shafranov, *Sov. Physics JETP*, vol. **6** (1958), 545.

REPORT DOCUMENTATION PAGE

Form Approved
OMB No. 0704-0188

1. AGENCY USE ONLY (*Leave blank*)

2. REPORT DATE
December 2000

3. REPORT TYPE AND DATES COVERED
Contractor Report

4. TITLE AND SUBTITLE
Theoretical Analysis of the Electron Spiral Toroid Concept

5. FUNDING NUMBERS
PO L-8871
WU 522-17-41-20

6. AUTHOR(S)
Jean-Luc Cambier and David A. Micheletti

7. PERFORMING ORGANIZATION NAME(S) AND ADDRESS(ES)
MSE Technology Applications, Inc.
200 Technology Way
P.O. Box 4078
Butte, MT 59702

8. PERFORMING ORGANIZATION REPORT NUMBER
NASA-32

9. SPONSORING/MONITORING AGENCY NAME(S) AND ADDRESS(ES)
National Aeronautics and Space Administration
Langley Research Center
Hampton, VA 23681-2199

10. SPONSORING/MONITORING AGENCY REPORT NUMBER
NASA/CR-2000-210654

11. SUPPLEMENTARY NOTES
Langley Technical Monitor: Dennis M. Bushnell

12a. DISTRIBUTION/AVAILABILITY STATEMENT
Unclassified-Unlimited
Subject Category 75 Distribution: Standard
Availability: NASA CASI (301) 621-0390

12b. DISTRIBUTION CODE

13. ABSTRACT *(Maximum 200 words)*
This report describes the analysis of the Electron Spiral Toroid (EST) concept being promoted by Electron Power Systems Inc. (EPS). The EST is described as a toroidal plasma structure composed of ion and electron shells. It is claimed that the EST requires little or no external confinement, despite the extraordinarily large energy densities resulting from the self-generating magnetic fields. The present analysis is based upon documentation made available by EPS, a previous description of the model by the Massachusetts Institute of Technology (MIT), and direct discussions with EPS and MIT. It is found that claims of absolute stability and large energy storage capacities of the EST concept have not been substantiated. Notably, it can be demonstrated that the ion fluid is fundamentally unstable. Although various scenarios for ion confinement were subsequently suggested by EPS and MIT, none were found to be plausible. Although the experimental data does not prove the existence of EST configurations, there is undeniable experimental evidence that some type of plasma structures whose characteristics remain to be determined are observed. However, more realistic theoretical models must first be developed to explain their existence and properties before applications of interest to NASA can be assessed and developed.

14. SUBJECT TERMS
Physics, Plasma Physics, Plasma Applications, Energy Storage, Propulsion

15. NUMBER OF PAGES
42

16. PRICE CODE
A03

17. SECURITY CLASSIFICATION OF REPORT
Unclassified

18. SECURITY CLASSIFICATION OF THIS PAGE
Unclassified

19. SECURITY CLASSIFICATION OF ABSTRACT
Unclassified

20. LIMITATION OF ABSTRACT
UL